A Section 508–conformant HTML version of this article is available at https://doi.org/10.1289/EHP6262.

Evaluating the Role of the Steroid and Xenobiotic Receptor (SXR/PXR) in PCB-153 Metabolism and Protection against Associated Adverse Effects during Perinatal and Chronic Exposure in Mice

Riann Jenay Egusquiza,[1] Maria Elena Ambrosio,[2] Shuyi Gin Wang,[2] Kaelen Marie Kay,[2] Chunyun Zhang,[3] Hans-Joachim Lehmler,[3] and Bruce Blumberg[1,2]

[1]Department of Pharmaceutical Sciences, University of California, Irvine, California, USA
[2]Department of Developmental and Cell Biology, University of California, Irvine, California, USA
[3]Department of Occupational and Environmental Health, University of Iowa, Iowa City, Iowa, USA

Background: Polychlorinated biphenyls (PCBs) are environmental toxicants; PCB exposure has been associated with adverse effects on wildlife and humans. However, the mechanisms underlying these adverse effects are not fully understood. The steroid and xenobiotic receptor [SXR; also known as the pregnane X receptor (PXR) and formally known as NR1I2] is a nuclear hormone receptor that regulates inducible metabolism of drugs and xenobiotics and is activated or inhibited by various PCB congeners.

Objectives: The aim of this study was to investigate the effects of exposure to PCB-153, the most prevalent PCB congener in human tissues, on SXR knockout mice (SXRKO) and to elucidate the role of SXR in PCB-153 metabolism and promotion of its harmful effects.

Methods: Wild-type (WT) and SXRKO mice were chronically or perinatally exposed to a low dose (54 μg/kg/d) of PCB-153. Blood, livers, and spleens were analyzed using transcriptome sequencing (RNA-seq) and molecular techniques to investigate the impacts of exposure on metabolism, oxidative stress, and hematological parameters.

Results: SXRKO mice perinatally exposed to PCB-153 displayed elevated oxidative stress, symptoms of hemolytic anemia, and premature death. Transcriptomal analysis revealed that expression of genes involved in metabolic processes was altered in SXRKO mice. Elevated levels of the PCB-153 metabolite, 3-OH-PCB-153, were found in exposed SXRKO mice compared to exposed WT mice. Blood hemoglobin (HGB) levels were lower throughout the lifespan, and the occurrence of intestinal tumors was larger in SXRKO mice chronically exposed to PCB-153 compared to vehicle and WT controls.

Discussion: Our results suggest that altered metabolism induced by SXR loss of function resulted in the accumulation of hydroxylated metabolites upon exposure to PCB-153, leading to oxidative stress, hemolytic anemia, and tumor development in a mouse model. These results support a major role for SXR/PXR in protection against xenobiotic-induced oxidative stress by maintaining proper metabolism in response to PCB-153 exposure. This role of SXR could be generally applicable to other environmental toxicants as well as pharmaceutical drugs. https://doi.org/10.1289/EHP6262

Introduction

Polychlorinated biphenyls (PCBs) are a class of environmental contaminants formerly widely used in industrial products, including plastics, adhesives, and electrical equipment (U.S. EPA 2015). Continued production of these chemicals was banned in the late 1970s due to evidence of harmful effects of exposure on human health (U.S. EPA 1979). These effects ranged from acute to developmental and included immunological responses (Weisglas-Kuperus et al. 1995, 2004), neurological abnormalities (Jacobson et al. 1990; Verner et al. 2015), and an increased risk for multiple types of cancer (Brody et al. 2007; Spinelli et al. 2007). Despite the ban on their production, PCBs are still found in the environment due to their high chemical stability (U.S. EPA 2015). Many PCB congeners are also resistant to biological degradation, which leads to bioaccumulation in animals (Muir et al. 1988; Rasmussen et al. 1990) and humans (Norström et al. 2010). The highest levels of human exposure to PCBs resulted from dietary consumption of contaminated food, mainly fish and poultry, and inhalation of contaminated air and house dust (Ampleman et al. 2015; Faroon et al. 2003; Norström et al. 2010).

PCBs were detected at high levels (between 0.5–4 mg/kg fat) in human breast milk, raising additional concerns about potential effects of exposure during development (DeKoning and Karmaus 2000; Faroon et al. 2003; Safe 1994). Associations were observed between prenatal and perinatal PCB exposure and reduced body weight (BW) (Chou et al. 1979; Fein et al. 1984; Jacobson et al. 1990b), immunological disruptions (Arena et al. 2003; Weisglas-Kuperus et al. 2004), and neurological abnormalities (Curran et al. 2011; Jacobson et al. 1990a, 1990b) that can lead to physiological and cognitive consequences later in life in both animals and humans. Their continued presence in humans (Ampleman et al. 2015; Čechová et al. 2017; Pirard et al. 2018; van den Berg et al. 2017), food sources (Barone et al. 2019; Bhavsar et al. 2007; Lüth et al. 2018), and indoor and outdoor air (Ampleman et al. 2015) indicates that PCBs are a still a current and persistent risk to the environment and future generations.

The mechanisms through which PCBs contribute to acute and lifelong effects following developmental exposure remain poorly understood. There are 209 PCB congeners that differ in the number and location of chlorine substituents. PCBs are often characterized into two groups based on similarity to 2,3,7,8-tetrachlorodibenzo-*p*-dioxin (TCDD, colloquially called dioxin), a known carcinogen. Like TCDD, dioxin-like PCBs (DL-PCBs) activate the aryl hydrocarbon receptor (AhR), which underlies many of their adverse health effects (Kafafi et al. 1993; Okey et al. 1994; Safe et al. 1985). Nondioxin-like PCBs (NDL-PCBs), which do not activate the AhR, also induce adverse effects *in vitro* (Ferrante et al. 2011; Hamers et al. 2011) and in animal exposure studies (Elnar et al. 2012; Haave et al. 2011; Strathmann et al. 2006). In addition, exposure to NDL-PCBs has been associated with harmful effects, such as cancers, in exposed humans (Engel et al. 2007; Spinelli et al. 2007). However, the underlying mechanisms for the adverse effects of NDL-PCBs remain largely uncharacterized, with most studies utilizing rodent models (Gaspar-Ramírez et al. 2015; Hamers et al. 2011; Lu et al.

Address correspondence to B. Blumberg, 2011 Biological Sciences 3, University of California, Irvine, CA 92697-2300 USA. Email: blumberg@uci.edu

Supplemental Material is available online (https://doi.org/10.1289/EHP6262).

B.B. is a named inventor on patents related to SXR. All other authors declare they have no actual or potential competing financial interests.

Received 21 September 2019; Revised 20 March 2020; Accepted 24 March 2020; Published 30 April 2020; Corrected 20 July 2020.

2004; Strathmann et al. 2006). Determining the mode of action of NDL-PCBs is important for treatment of exposed individuals and to understand the action of alternative chemicals with similar structures [e.g., polybrominated biphenyls (PBBs) and polybrominated diphenyl ethers (PBDEs)] that may act through the same pathways and induce similar adverse effects.

Some NDL-PCBs have been demonstrated to interfere with estrogen and androgen signaling in CHO and MCF7 cells (Bonefeld-Jørgensen et al. 2001) and alter thyroid signaling in rodents (Giera et al. 2011; Ness et al. 1993). This could possibly explain some of the adverse reproductive consequences observed in animals exposed to NDL-PCB congeners or mixtures (Hsu et al. 2007). However, the mechanisms underlying the ability of these chemicals to induce tumor progression, alter immune processes, and increase risk for various cancers in exposed individuals are still not fully understood. It has been proposed that oxidative stress elicited by PCBs and PCB metabolites may be a contributing factor in their observed carcinogenicity (Oakley et al. 1996). The steroid and xenobiotic receptor (SXR), also known as the pregnane X receptor (PXR) and formally known as NR1I2, is a nuclear hormone receptor expressed at high levels in the liver and intestine and at lower but detectable levels in most other tissues (Blumberg et al. 1998; Miki et al. 2005). When it is activated by ligands (drugs and endobiotic and xenobiotic chemicals), SXR/PXR up-regulates expression of genes encoding enzymes involved in all three phases of xenobiotic metabolism: phase I enzymes such as cytochrome P450 (CYPs), phase II conjugating enzymes such as glutathione S-transferase (GST), and phase III drug transporters (Blumberg et al. 1998; Geick et al. 2001; Xie et al. 2000b). Predictably, SXR knockout (SXRKO) mice displayed defects in inducible xenobiotic metabolism, making them hypersensitive to the effects of certain xenobiotics (Wei et al. 2002; Xie et al. 2000a). Some NDL-PCBs have been demonstrated to both activate and inhibit SXR and subsequently affect its activity in *in vitro* studies (Al-Salman and Plant 2012; Gährs et al. 2013; Hurst and Waxman 2005; Tabb et al. 2004; Zhang et al. 2008). However, relatively little is known about the role of SXR in NDL-PCB metabolism or mechanisms of action *in vivo*.

PCB-153 (2,2′,4,4′,5,5′-hexachlorobiphenyl) is a highly chlorinated NDL-PCB that was reported to be the most prevalent congener found in human tissue and breast milk (Safe 1994) and in contaminated fish (Looser and Ballschmiter 1998; Lüth et al. 2018). PCB-153 was also shown to increase tumor incidence in rodents (Strathmann et al. 2006) and was associated with an increased risk for non-Hodgkin's lymphoma (Engel et al. 2007; Spinelli et al. 2007) and other cancers (Brody et al. 2007; Hardell et al. 2006; Strathmann et al. 2006) in exposed humans. PCB-153 was reported to be the most potent NDL-PCB congener on SXR induction of target genes in some human cell lines (Al-Salman and Plant 2012) and rat hepatocytes (Gährs et al. 2013). The current study aimed to investigate the effects of exposure to PCB-153 in mice lacking SXR/PXR and to assess the role of this receptor in modulating the toxic effects of PCB-153 *in vivo*.

Methods

Animal Maintenance

Wild-type (WT), SXRKO, and humanized SXR knock-in (hSXRki) mice were maintained and housed at the University of California, Irvine (UCI). C57BL/6J WT mice were purchased from Jackson Labs and maintained in our lab for at least five generations before being used for experiments. SXRKO mice were descendants from a colony of SXRKO (129SVEV) mice from the Salk Institute (a gift of Professor Ron Evans) and were backcrossed onto the C57BL/6J background for six generations to obtain SXRKO mice with an essentially pure C57BL/6J background. hSXRki mice were descendants from a colony of hSXRki mice (C57BL/6 CrSlc) from the National Institute of Health Sciences, Japan (a gift from Professor Jun Kanno) (Igarashi et al. 2012) and were backcrossed onto the C57BL/6J background for six generations. Mice were housed in microisolator cages at four to five mice per cage in a temperature-controlled room (23–25°C) with a 12-h light/dark cycle. Water and food (5P14 ProLab RMH 2500; LabDiet) were provided *ad libitum*. Animals were treated humanely, and all procedures were approved by the Institutional Animal Care and Use Committee of UCI.

PCB-153 Exposure

PCB-153 was purchased from ChemService Inc. Stock solutions were prepared at 20 mM in dimethylsulfoxide (DMSO). Stocks were further diluted in DMSO to 1 mM concentration and stored at −80°C until use. Chemical exposure was administered via the drinking water. Mice received 1 μM PCB-153 or vehicle (0.1% DMSO) in 0.5% carboxymethylcellulose prepared in autoclaved tap water. Water containing PCB-153 or vehicle was replaced twice weekly. WT and SXRKO females (8–10 wk old) were randomly assigned to exposure groups (DMSO or PCB-153). In a separate experiment, SXRKO and hSXRki females (8–18 wk old) were randomly assigned to exposure groups (DMSO or PCB-153). For all studies, females were exposed 3 d prior to breeding; exposure was removed for mating. Exposed females were bred with unexposed males of the same genotype (1 male to 1 female). PCB-153 or vehicle exposure was resumed for the females following 3 d of mating and then continued throughout pregnancy and lactation. Breeding efficiencies and pup numbers are listed in Table S1. Male offspring were toe clipped with a unique code at 7 d old in order to track possible effects related to the litter and to monitor each individual mouse through multiple time points. Male offspring were then weaned at 21 d with four to five pups per cage, each mouse coming from a different litter to prevent cage effects. The male offspring continued on the exposure they received perinatally via drinking water until euthanasia at 4 wk of age for perinatal exposure study or 10 months/45 wk of age for chronic exposure study (Figure 1A). Two independent perinatal exposure studies were conducted with WT ($n = 18$ total F0 female mice) and SXRKO ($n = 13$ total F0 female mice). Two independent chronic exposure studies were conducted with WT ($n = 20$ total F0 female mice) and SXRKO ($n = 19$ total F0 female mice), and a third chronic exposure study was conducted with hSXRki ($n = 16$ F0 female mice) and SXRKO ($n = 16$ F0 female mice). Since exposure was continued after weaning, it was not distinguishable if results were due to perinatal or postweaning exposure; therefore, offspring were analyzed as individuals instead of by litter. All male offspring were investigated for determining body and tissue weights, percentages of erythroid precursors, and lifespan complete blood counts. One male per litter was used for transcriptome sequencing (RNA-seq) analysis, malondialdehyde (MDA) measurements, reduced glutathione (GSH)/oxidized glutathione (GSSG) level determination, and quantitative real-time polymerase chain reaction (qPCR) validation of RNA-seq results to avoid potential litter effects. End points using only one individual from each litter are noted in the individual method sections. Female offspring were included in one cohort of the chronic exposure study but did not display any phenotype or abnormalities (data not shown). Therefore, female offspring were not investigated for the 4-wk-old perinatal exposure study or other cohorts of the chronic exposure study.

The dose of PCB-153 used in this study is equivalent to 0.15 μmol/kg/d or 54 μg/kg/d, assuming that mice consumed 1.5 mL/10 g of BW of water a day (Johns Hopkins University Animal Care and Use Committee 2019). The no observed adverse effect level (NOAEL) for PCB-153 for rodents is between 1 and

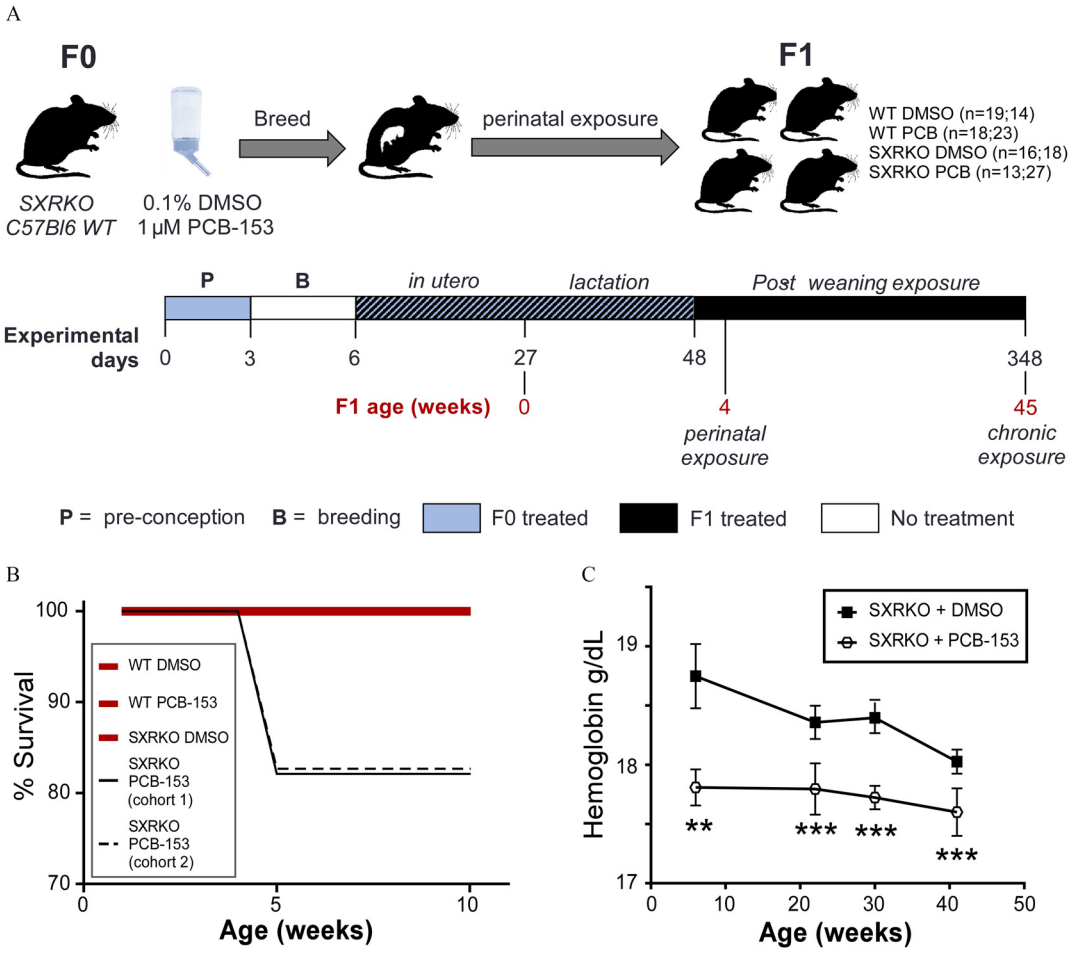

Figure 1. Experimental setup, survival, and blood hemoglobin analysis of wild-type (WT) and steroid and xenobiotic receptor knockout (SXRKO) mice exposed to polychlorinated biphenyl 153 (PCB-153) or vehicle. (A) Exposure schematic for perinatal and chronic exposure to PCB-153; number of mice per group are reported as (n = number of mice for perinatal study; number of mice for chronic study). (B) Survival of WT or SXRKO mice exposed to PCB-153 or vehicle [dimethylsulfoxide (DMSO)] in chronic exposure study; both cohorts of SXRKO mice exposed to PCB-153 are shown independently (cohort 1, $n = 16$; cohort 2, $n = 11$); all other groups are shown as the sum of both cohorts (WT DMSO, $n = 14$; WT PCB, $n = 23$; SXRKO DMSO, $n = 18$) and merged together in one bold red line. (C) Hemoglobin measurements of SXRKO mice exposed to DMSO ($n = 18$) or PCB-153 ($n = 22$) throughout lifespan in chronic exposure study, plotted as mean ± standard error of the mean (SEM). $^{**}p < 0.01$; $^{***}p < 0.001$ determined by Student's t-test.

125 mg/kg/d depending on the biological end point investigated (European Food Safety Authority 2005). The worst-case, environmentally relevant dose of PCB-153 for human exposure is 1.7 µmol/kg/d (Haave et al. 2011). We chose the dose of 0.15 µmol/kg/d (54 µg/kg/d) because it is relevant to human exposure levels and it is five times lower than the rodent NOAEL.

Complete Blood Count

Whole blood (50 µL) was collected bimonthly into heparinized capillary tubes from the saphenous vein for WT (DMSO, $n = 14$; PCB-153, $n = 23$) and SXRKO (DMSO, $n = 18$; PCB-153, $n = 22$) mice beginning at 6 wk until 9 months of age. Blood parameters were measured on a scil Vet ABC Hematology Analyzer (scil Animal Care Company) within 4 h of blood collection. Blood parameters measured included white blood cell count (WBC), red blood cell count (RBC), hematocrit (HCT), hemoglobin (HGB), mean corpuscular volume, mean cell HGB, mean corpuscular HGB concentration, RBC distribution width (RDW), platelet count, lymphocyte count, monocyte count, and granulocyte count.

Tissue and Cell Collection

Mice were euthanized by isoflurane overdose. Whole blood was collected by cardiac puncture. Aliquots of whole blood (20 µL) were flash frozen and stored at −80°C until further analysis. Remaining blood was centrifuged (2,000 × g at 4°C for 10 min) to separate cells from the plasma. Plasma was removed and stored at −80°C. Livers and spleens were dissected, flash frozen in liquid N_2, and stored at −80°C. A section of each spleen was set aside before flash freezing for splenocyte isolation.

Tumor Histology

Intestinal tumors were fixed in buffered 3.7% formaldehyde, embedded in paraffin, sectioned at 4–5 µm, and stained with hematoxylin and eosin by the core facility of the Department of Pathology and Laboratory Medicine at UCI, following standard protocols. An Axiovert 40 CFL microscope (Zeiss) (40× magnification) was used to acquire bright-field photomicrographs.

Spleen and Bone Marrow Cell Isolation

Spleens were physically dissociated using a petri dish and syringe plunger in 1 mL of cold phosphate-buffered saline (PBS) containing 1% fetal bovine serum (FBS) (Omega Scientific). Hind legs were dissected, tibias and femurs were isolated, and bone marrow cells were extracted by flushing cold PBS + 1% FBS buffer into the marrow cavity using a 25-gauge needle. Erythrocytes were lysed by incubating cell suspensions in ACK lysis buffer (150 mM NH_4Cl +

10 mM $KHCO_3$ + 0.1 mM Na_2 ethylenediaminetetraacetic acid) for 5 min. Cells were washed and resuspended in fluorescence-activated cell sorter (FACS) buffer (PBS + 1% FBS + 0.02% sodium azide) for flow cytometry antibody staining.

Flow Cytometry Analysis

Splenic and bone marrow cells were diluted in cold FACS buffer (PBS + 1% FBS + 0.02% sodium azide), divided into 4×10^4 cell aliquots, stained with an antibody cocktail of 1:200 APC anti-mouse TER119 (TONBO biosciences, catalog no. 20-5921-U025); 1:1,000 CD71, PE (eBioscience; catalog no. 12-0711-81); and 1:400 Alexa Fluor® 700 anti-mouse CD45 (BioLegend; catalog no. 103128) in the dark for 30 min at 4°C. Cells were analyzed on a BD LSRFortessa™ X-20 cytometer (BD Biosciences), and data were processed using FlowJo software (v10.5.3; Tree Star).

Erythrocyte Malondialdehyde/Lipid Peroxidation Measurement

Flash frozen blood samples ($n = 5$ per group, each coming from a different litter with the exception of SXRKO PCB-153, which has five mice coming from four litters) were mixed with 1 mL of sterile, ultrapure water [ultrafiltered, ultraviolet sterilized water from a Nanopure™ ultrapure water system (Barnstead International), hereafter called nanopure water] for 2 min to lyse the RBCs. RBC membranes were pelleted [12,000 × *g* for 5 min at room temperature (RT)] and supernatants discarded. RBC membranes were washed with nanopure water and pelleted again. MDA levels were obtained using the Lipid Peroxidation (MDA) Assay Kit (Sigma-Aldrich) following the manufacturer's protocol. Supernatants were plated in two technical replicates and measured on a fluorescence plate reader with excitation at 532 nm and emission at 553 nm.

Hemoglobin Measurement

Flash frozen blood samples ($n = 5$ per group, each coming from a different litter with the exception of SXRKO PCB-153, which has five mice coming from four litters) were diluted 1:200 in nanopure water. HGB content was determined using the Hemoglobin Assay Kit (Sigma-Aldrich) according to the manufacturer's protocol. Briefly, 50 μL of diluted blood was plated in a clear 96-well plate using two technical replicates for each sample. The assay reagent (200 μL) was added to each sample and incubated for 5 min at RT. The colorimetric products were measured at 400 nm.

GSH/GSSG Level Determination

Flash frozen blood samples ($n = 5$ per group, each coming from a different litter with the exception of SXRKO PCB-153, which has five mice coming from four litters) were diluted with 500 μL of nanopure water and deproteinized using one-fifth volume of 100% trichloroacetic acid (Sigma-Aldrich) and then centrifuged at 12,000 × *g* for 5 min at 4°C. Supernatants were neutralized by slowly adding sodium bicarbonate until the pH was equal to 4–6. GSH and total glutathione levels were determined using the GSH/GSSG Ratio Detection Assay Kit (Abcam) according to the manufacturer's protocol. Briefly, 25 μL of neutralized supernatants were plated in a black 384-well plate with a clear bottom using two technical replicates for both the GSH and total glutathione panels of each sample. The GSH assay mixture (25 μL) was added to the GSH panel, and the total glutathione assay mixture (25 μL) was added to the total glutathione panel and incubated for 30 min at RT in the dark. The fluorometric products were excited at 490 nm and emission measured at 520 nm. Concentrations of GSH and total glutathione were calculated by comparing to a standard curve.

Ex Vivo *Hemolysis Assay*

Blood was collected from untreated 4-wk-old WT and SXRKO mice ($n = 3$) by cardiac puncture using a needle and heparinized syringe. Blood was centrifuged (10 min at 5,000 rpm) and plasma was removed. Packed erythrocytes were washed twice with 1 × PBS (pH 7.4) and then diluted 1:50 in 1 × PBS (pH 6.2). A more acidic pH was used in the experimental buffer to obtain higher sensitivity to agent-induced hemolysis (Evans et al. 2013). RBCs were treated with 10, 5, 2.5, or 1.25 μM of PCB-153 or with a positive control [1% sodium dodecyl sulfate (SDS)] in a round-bottom 96-well plate with a final volume of 100 μL for 2 h at 37°C. Two technical replicates were performed for each sample. After incubation, cells were pelleted, and supernatants were transferred to a clear 96-well plate. Absorbance of free heme in the supernatant was measured at 405 nm.

RNA Extraction

Frozen tissue sections were homogenized rapidly in 1 mL of Trizol reagent (Thermo Fisher Scientific). RNA was isolated from the tissue–Trizol homogenate by chloroform extraction. RNA was precipitated with an equal volume of 100% isopropanol and centrifuged, and salt was removed by washing with 70% ethanol. The final RNA product was resuspended in DNase/RNase-free nanopure water and quantified by spectrophotometry, and its integrity was verified by denaturing agarose gel electrophoresis.

RNA-Seq Library Prep and Sequencing

Five samples from each exposure group, each coming from a different litter with the exception of SXRKO PCB-153, which has five mice coming from four litters, were randomly selected for RNA-seq analysis. The two SXRKO PCB-153 mice coming from the same litter are labeled KP2 and KP3. Both liver and spleen transcriptomes were analyzed for each selected sample. The extracted RNA was further purified using a Quick-RNA™ Microprep Kit (Zymo Research). RNA quality, quantity, and integrity were measured with the Bioanalyzer 2100 (Agilent); results are shown in Supplemental Material, "RNA quality." RNA-seq libraries were prepared by the UCI Genomics High Throughput Facility using 1 μg of RNA and the TruSeq Stranded mRNA Library Prep Kit (Illumina). Two separate libraries were made for the liver and spleen samples with 20 samples each using Illumina reagents. Each library was sequenced on a HiSeq4000 (Illumina) instrument using single-stranded 100-bp read length, with one library per flow cell lane. We obtained an average of 18.6 ± 2.6 million reads per sample.

RNA-Seq Analysis and Visualization

Sequence quality was checked in the Fastq files using FastQC (v0.11.8; Babraham Bioinformatics). Fastq files were then aligned to the mouse MM10 genome assembly (ENSEMBL) using the STAR aligner (Dobin et al. 2013) on the UCI High Performance Computing Cluster (hpc.oit.uci.edu/). The resulting BAM files were also checked with FastQC. The average number of uniquely mapped reads was 84.7 ± 2.3%. Spleen sample WD2 was removed from downstream analysis due to lower mapping quality (76.1%) compared to all other spleen samples. Reads were counted using Rsubread/featureCounts [Bioconductor package in R (v3.5.5; R Development Core Team)] (Liao et al. 2014), and differential expression analysis was conducted using DESeq2 [Bioconductor package in R (R Development Core Team)] (Love et al. 2014). Differentially expressed genes (DEGs) were selected using a Benjamini-Hochberg-adjusted *p*-value (*p*-adj) of <0.05 and absolute value $[\log_2 \text{fold change (FC)}] > 0.3$. Normalized counts obtained from DESeq2 analysis were used to generate heatmaps. Heatmaps

were plotted using the pheatmap package in R. Lists of significant only DEGs with foldchange and *p*-adj values are provided in Excel Tables S1 and S2. Raw and processed RNA-seq data files, including full lists of DEGs, are available at Gene Expression Omnibus (GSE135916). The HPC and R scripts used for RNA-seq analysis are shown in the Supplemental Material, "RNA-seq script."

Gene Ontology Analysis

DEGs obtained from DESeq2 were input into MouseMine (Mouse Genome Informatics 2019) using a Benjamini-Hochberg-corrected *p*-value of <0.05 to determine significance. For gene ontology (GO) term enrichment, terms were reduced to 25 terms using Revigo (Supek et al. 2011) and independent selection of desired terms. GO term enrichment plots were made using the ggplot2 package in R (R Development Core Team). Enrichment is plotted as $(\text{no. of DEGs within the term})/(\text{total no. of genes in the term}) \times 100$. A full list of significant GO terms in provided in Excel Tables S3 and S4.

qPCR Validation of Differentially Expressed Genes

Complementary DNA (cDNA) was synthesized using 2 μg of extracted intact RNA and Superscript™ III Reverse Transcriptase (Thermo Fisher Scientific) according the manufacturer's protocol. Synthesized cDNA was diluted 5-fold for qPCR analysis. Diluted cDNA was combined with SYBR™ Green qPCR Master Mix (Thermo Fisher Scientific) and the primer mix for gene of interest and analyzed using a LightCycler® 480 (Roche). Two technical replicate cycle threshold (Ct) values were averaged for each biological replicate. Mean Ct values were normalized to Rplp0 ribosomal protein, large, P0 (36B4/Rplp0) or Beta-actin (Actb) for liver or spleen, respectively, and relative FC mRNA levels were then calculated by using the ΔΔCt method (Livak and Schmittgen 2001) with relative gene expression presented as mean FC over vehicle control ± standard error of the mean. Primers were designed using PerlPrimer software (v1.1.21; Owen Marshall), and oligonucleotides were purchased from Sigma-Aldrich. qPCR primer sequences are given in Table S2.

Extraction of PCB-153 and 3-OH-PCB 153 from Liver

Liver samples were processed following a published procedure (Milanowski et al. 2010). Briefly, samples (247 ± 62 mg) were spiked with PCB 117 and 4′-OH-PCB 159 (50 ng each) as surrogate recovery standards. After homogenization in 2-propanoal (3 mL), samples were extracted with diethyl ether (1 mL) and hexane:diethyl ether (9:1 vol/vol; 2.5 mL). The combined extracts were washed with phosphoric acid (0.1 M solution in 0.9% aqueous sodium chloride, 5 mL) and derivatized with diazomethane (0.5 mL) overnight at 4°C. Sulfur removal and sulfuric acid treatment steps were employed before analysis as described (Kania-Korwel et al. 2005).

Extraction of PCB-153 and 3-OH-PCB-153 from Plasma

Plasma samples (71 ± 51 mg) were spiked with PCB-117 and 4′-OH-PCB-159 (50 ng each) as surrogate recovery standards and denatured with hydrochloric acid (6 M; 1 mL) and 2-propanol as reported previously (Kania-Korwel et al. 2011; Wu et al. 2011). All samples were extracted with hexane:methyl *tert*-butyl ether (1:1 vol/vol; 5 mL) and then reextracted with hexane (3 mL). The combined organic extracts were washed with potassium chloride solution (1%; 4 mL) and underwent the derivatization and cleanup procedures as above.

Quantitation of PCB-153 and 3-OH-PCB-153

Quantitative analyses of PCB-153 and 3-OH-PCB 153 in sample extracts were carried out on a 7890A gas chromatography (GC) system (Agilent) equipped with a SPB®-1 capillary column (60 m × 250 μm × 0.25 μm film thickness; Supelco) and a ^{63}Ni-micro electron capture detector (Agilent) as previously reported (Wu et al. 2011), with minor modifications and described below. Helium was used as carrier gas with a constant flow rate of 2 mL/min. The injector and detector temperatures were 240°C and 300°C, respectively. The column temperature program was initially set as 50°C, held for 1 min, then gradually increased to 200°C by 30°C/min, increased to 250°C by 1°C/min, increased to a final temperature of 280°C by 10°C/min, and held there for 3 min. The PCB-153 and 3-OH-PCB-153 were identified by the retention time of their authentic standards. The relative retention time (RRT) of all analytes was within 0.5% of the RRT of the respective standard. PCB 153 and 3-OH-PCB 153 were quantified with the internal standard method as described (Kania-Korwel et al. 2007). Levels were corrected for recoveries below 100%.

Quality Assurance/Quality Control of PCB-153 and 3-OH-PCB-153 Measurements

The responses of PCB-153 ($R^2 = 0.999$), 3-OH-PCB-153 ($R^2 = 0.999$), PCB-117 (recovery standard; $R^2 = 0.999$), 4′-OH-PCB-159 (recovery standard, $R^2 = 0.999$), and PCB-204 (internal standard; $R^2 = 0.999$) on the GC–electron capture detector were linear from 1 to 1,000 ng/mL. The limits of detection (LODs) of PCB-153 and 3-OH-PCB-153 were calculated from method blanks as $\text{LOD} = \text{mean blanks} + k \times \text{standard deviation blanks}$ (k is the Student's t-value for a degree of freedom of $n - 1 = 5$ for liver and $n - 1 = 5$ for serum at the 99% confidence level). The LODs for analyses of liver samples were 0.09 ng and 0.03 ng for PCB-153 and 3-OH-PCB-153, respectively. The LODs for analyses of serum samples were 0.11 ng and 0.07 ng for PCB-153 and 3-OH-PCB-153, respectively. The background levels of PCB-153 and 3-OH-PCB-153 in control liver samples were 0.15 ± 0.07 ng/g ($n = 19$) and 0.11 ± 0.03 ng/g ($n = 19$), respectively. The background levels of PCB-153 and 3-OH-PCB-153 in control serum samples were 0.83 ± 1.64 ng/g ($n = 18$) and 0.85 ± 2.38 ng/g ($n = 18$), respectively. The recoveries of PCB-153 and 3-OH-PCB-153 spiked into control liver samples were 78 ± 6% (range: 73–87%; $n = 5$) and 86 ± 9% (range: 78–99%; $n = 5$), respectively. The recoveries of PCB-153 and 3-OH-PCB-153 spiked into control serum samples were 83 ± 6% (range: 74–90%; $n = 6$) and 70 ± 17% (range: 51–102%; $n = 6$), respectively. For liver analyses, the recoveries of the surrogate standards added to every samples were 95 ± 12% (range: 55–111%; $n = 40$) and 91 ± 14% (range: 56–120%; $n = 40$) for PCB-117 and 4′-OH-PCB-159, respectively. For serum analyses, the recoveries of the surrogate standards added to every samples were 88 ± 8% (range: 74–102%; $n = 47$) and 99 ± 14% (range: 59–120%; $n = 47$) for PCB-117 and 4′-OH-PCB-159, respectively.

Statistical Analysis

Data visualization and statistical analyses were conducted in Prism (version 8; GraphPad), excluding RNA-seq analysis, which was completed in R and other software packages as indicated above. Thirteen to 27 biological replicates were used for exposure experiments and *in vivo* and FACS analyses. Downstream biochemical analyses, RNA-seq analysis, and qPCR gene validations used five biological replicates per group. Two-way analysis of variance with Tukey's multiple-comparisons test or Student's *t*-test were used to determine statistical differences between

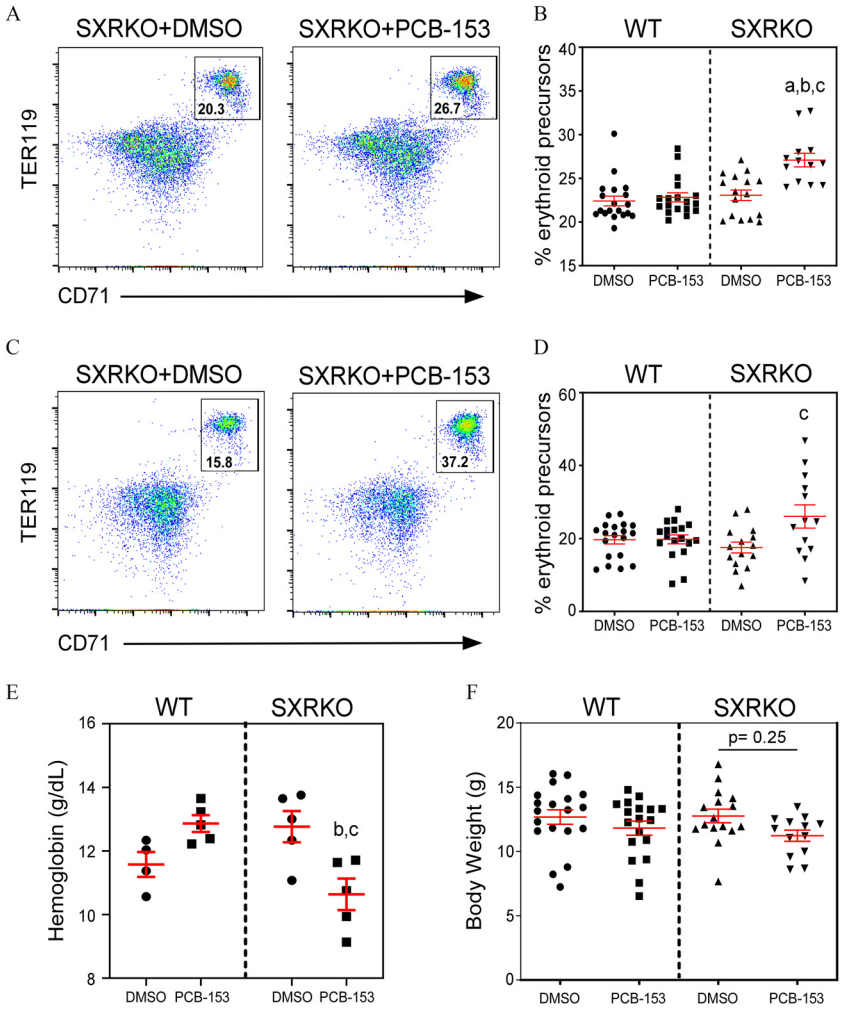

Figure 2. Erythroid precursors, blood hemoglobin, and body weights of 4-wk-old wild-type (WT) and steroid and xenobiotic receptor knockout (SXRKO) mice perinatally exposed to polychlorinated biphenyl 153 (PCB-153) or vehicle. Representative fluorescence-activated cell sorter (FACS) plots of (A) bone marrow or (C) spleens of SXRKO mice exposed to dimethylsulfoxide (DMSO) and PCB-153, gating on erythroid precursors. Quantifications of erythroid precursors in (B) bone marrow and (D) spleens of 4-wk-old perinatally exposed mice (WT DMSO, $n = 19$; WT PCB, $n = 18$; SXRKO DMSO, $n = 16$; SXRKO PCB, $n = 13$) plotted as mean ± standard error of the mean (SEM). (E) Blood hemoglobin levels of WT and SXRKO mice at 4 wk of age perinatally exposed to either DMSO or PCB-153 ($n = 5$ per group) plotted as mean ± SEM. (F) Body weights of exposed mice at 4 wk of age (WT DMSO, $n = 19$; WT PCB, $n = 18$; SXRKO DMSO, $n = 16$; SXRKO PCB, $n = 13$) plotted as mean ± SEM. a, statistically significant compared to WT DMSO; b, statistically significant compared to WT PCB; c, statistically significant compared to SXRKO DMSO determined by two-way analysis of variance (ANOVA) and Tukey's multiple-comparisons test.

groups. The test used for each analysis is stated in the figure descriptions. A p-value of <0.05 was considered statistically significant for all assays other than RNA-seq analysis, which used adjusted p-values based on the Benjamini-Hochberg test.

Results

Number of Fatalities and Blood Hemoglobin Values of Wild-Type and SXRKO Mice Chronically Exposed to a Low Dose of PCB-153

WT and SXRKO females were exposed to approximately 54 μg/kg BW/d of PCB-153 or vehicle (0.1% DMSO) in the drinking water throughout pregnancy and lactation. Male offspring were continued on the same exposure after being weaned from the mother until either 4 wk or 10 months (45 wk) of age and were monitored to investigate the role of SXR/PXR on the action of developmental and chronic exposure to an NDL-PCB (Figure 1A).

We observed premature death at 5 wk of age in approximately 18% of male SXRKO offspring from the PCB-153 group in two independent experimental cohorts of the chronic exposure study; no deaths were observed in the vehicle-exposed SXRKO mice or in any of the WT exposure groups (Figure 1B; Table S3). Necropsy revealed no obvious causes of death (data not shown), and no additional deaths occurred after this age (Figure 1B). Blood parameters were monitored every 9–10 wk in mice that survived after 5 wk of age. Lower HGB levels were observed at 6 wk of age in PCB-153-exposed compared to vehicle (DMSO)-exposed SXRKO mice (Figure 1C). SXRKO mice chronically exposed to PCB-153 consistently displayed lower blood HGB values throughout their lifespan compared to DMSO-exposed SXRKO mice. Interestingly, the largest differences between DMSO- and PCB-153-exposed SXRKO mice were observed at younger ages; the differences at older ages appear to be due to higher HGB levels in vehicle-exposed SXRKO animals (Figure S1B). There were no differences between the exposure groups among WT mice at any age (Figure S1A; Table S4). No other blood parameters were consistently different between groups, although lower HCT and higher RDW were transiently observed in PCB-153-exposed SXRKO mice at 6 wk of age compared to vehicle-exposed SXRKO mice (Table S5).

Analysis of Bone Marrow and Spleen from 4-Wk-Old Mice Perinatally Exposed to PCB-153 for Signs of Erythropoiesis and Hematological Abnormalities

To further investigate the cause of death that occurred at 5 wk of age in the PCB-153-exposed SXRKO mice and the possible connection to the lower blood HGB values, we conducted a perinatal exposure study to investigate F1 offspring at 4 wk of age and focused our investigation on the tissues involved in the production of RBCs and iron homeostasis: blood, bone marrow, spleen, and liver.

A higher percentage of erythroid precursors (TER119+, CD71+), the progenitors of RBCs, was observed in the bone marrow and spleen via FACS analysis in SXRKO mice perinatally exposed to PCB-153 at 4 wk of age (Figure 2A–D). No differences were observed between exposure groups for WT mice (Figure 2B,D). This higher percentage of erythropoiesis was accompanied by lower blood HGB levels for PCB-153-exposed SXRKO mice compared to vehicle-exposed SXRKO mice (Figure 2E), consistent with our observations performed in older animals (Figure 1C). Interestingly, WT mice showed a trend for higher blood HGB levels with PCB-153 exposure at 4 wk of age (Figure 2E); however, this was not significant and not observed at any other age (Figure S1A). PCB-153-exposed SXRKO offspring also displayed smaller BWs at 4 wk of age compared to vehicle-exposed and WT controls, although this was not statistically significant (Figure 2F). There were no differences in relative spleen or liver weights for exposed pups or dams (Figure S2).

Since the spleen is the site of stress erythropoiesis (Paulson et al. 2011) and because it is involved in the filtering and recycling of RBCs, we conducted RNA-seq analysis to evaluate alterations in splenic gene expression between PCB-153- and vehicle-exposed WT and SXRKO mice. Numerous differences were observed between PCB-153 and DMSO perinatally exposed SXRKO mice, encompassing 380 GO biological processes terms (Table 1). Significant enrichments were found in terms that included heme metabolism, cell cycle, and immune system pathways (Figure S3; Excel Table S3). Compared to vehicle-exposed SXRKO mice, PCB-153-exposed SXRKO mice displayed higher expression of genes related to erythroid development, supporting the phenotypic finding of higher splenic erythropoiesis (Figure 3A). Kruppel-like factor 1 (*Klf1*), a transcription factor important for erythroid lineage commitment and erythrocyte maturation (Siatecka and Bieker 2011), had significantly higher gene expression in SXRKO mice exposed to PCB-153 compared to DMSO, and this expression pattern was validated by qPCR (Figure 3B). Several other key DEGs for this pathway were validated with qPCR analysis (Figure S4). PCB-153-exposed SXRKO mice also displayed elevated expression of genes related to heme metabolism compared to DMSO-exposed SXRKO mice (Figure 3C). This included important components in heme synthesis, such as ferrochelatase (*Fech*) (Figure 3C; Figure S4B), which encodes for the terminal enzyme of the heme biosynthesis pathway (Ferreira 1999), and biliverdin reductase B (*Blvrb*) (Figure 3C,D), which encodes for one of the most important enzymes involved in the catabolism of free heme (Barañano et al. 2002). Selected DEGs in this GO term were validated by qPCR (Figure S4). The expression levels of genes in these GO terms correlated with the observed level of splenic erythropoiesis (Figure S5). No differences in mRNA expression for all genes investigated were observed between exposure groups for WT mice (Figure 3B,D; Figure S4). Since we observed DEGs between PCB-153- and vehicle-exposed

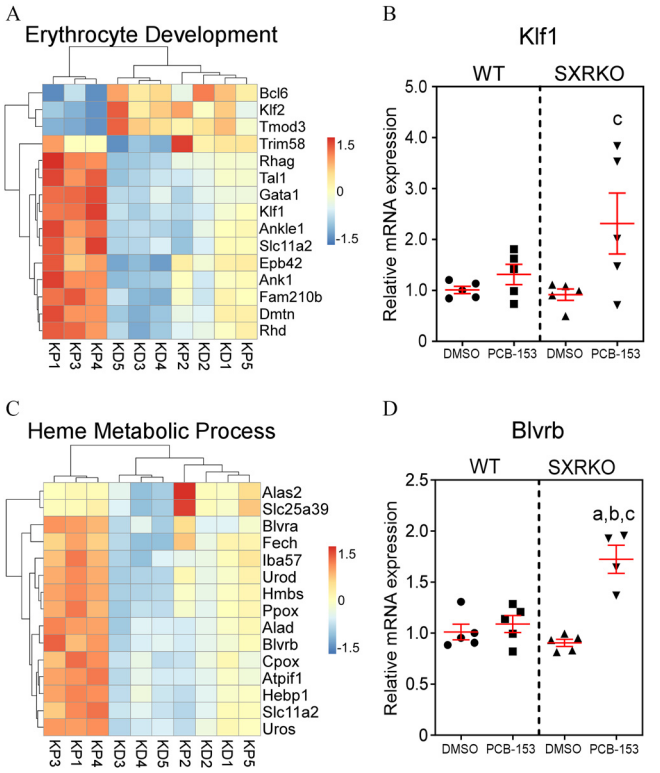

Figure 3. Differentially expressed genes in erythrocyte development and heme metabolism in the spleen between steroid and xenobiotic receptor knockout (SXRKO) mice perinatally exposed to polychlorinated biphenyl 153 (PCB-153) and vehicle. (A) Differentially expressed genes (DEGs) involved in erythrocyte development in the spleen of SXRKO mice exposed to PCB-153 compared to SXRKO mice exposed to dimethylsulfoxide (DMSO). (B) Kruppel-like factor 1 (*Klf1*) erythroid transcription factor quantitative real-time polymerase chain reaction (qPCR) gene expression analysis ($n = 5$ per group). (C) Heatmap of DEGs related to heme metabolism in the spleen of SXRKO mice exposed to PCB-153 compared to SXRKO mice exposed to DMSO. (D) Biliverdin B (*Blvrb*) qPCR gene expression analysis ($n = 5$ per group) in the spleens of WT and SXRKO mice exposed to DMSO or PCB-153. qPCR data plotted as mean fold change over WT DMSO ± standard error of the mean (SEM). a, statistically significant compared to WT DMSO; b, statistically significant compared to WT PCB; c, statistically significant compared to SXRKO DMSO determined by two-way analysis of variance (ANOVA) and Tukey's multiple-comparisons test. Note: D, DMSO exposure; K, SXRKO mice; P, PCB-153 exposure; W, WT mice.

Table 1. Spleen transcriptome sequencing (RNA-seq) results.

	SXRKO DMSO vs. WT DMSO	SXRKO PCB vs. WT PCB	SXRKO PCB vs. SXRKO DMSO	WT PCB vs. WT DMSO
Total DEGs	23	198	1,598	4
Up-regulated	16	125	965	1
Down-regulated	7	73	633	3
GO terms (BPs)	0	24	380	0

Note: Number of total, up-regulated, and down-regulated differentially expressed genes (DEGs) for each comparison and the resulting number of significant gene ontology (GO) terms for biological processes (BPs). DEGs were determined by DESeq2 with adj p-adj < 0.05 and absolute value of log2 [fold change (FC)] > 0.3. GO term significance determined by Benjamini-Hochberg correction test (p-adj < 0.05) in MouseMine (Mouse Genome Informatics 2019). DMSO, dimethylsulfoxide; PCB, polychlorinated biphenyl-153; SXRKO, steroid and xenobiotic receptor knockout (SXRKO); WT, wild-type.

SXRKO spleens, we asked whether PCB-153 was directly inducing damage on RBCs. To answer this, we isolated RBCs from WT and SXRKO mice and exposed them *ex vivo* to varying concentrations of PCB-153 alongside positive (SDS) and negative (DMSO) controls. Interestingly, we did not observe any direct hemolytic activity of PCB-153 on RBCs from either WT or SXRKO animals (Figure S6).

Investigating Oxidative Stress in the Spleens and Red Blood Cells of Wild-Type and SXRKO Mice Perinatally Exposed to PCB-153

In addition to elevated heme synthesis and erythroid development, transcriptomal analysis of the spleens revealed enrichment for genes in GO terms related to oxidative stress (Figures S3 and S7A). Compared to vehicle-exposed SXRKO mice, SXRKO mice perinatally exposed to PCB-153 had a different expression profile for genes involved in responses to reactive oxygen species (ROS), with higher expression of key antioxidant genes, including peroxiredoxin 2 (*Prdx2*) and glutathione peroxidase 1 (*Gpx1*) (Figure 4A; Figure S7A,B), and the transcription factor *Foxo3* (Figure S7A), which is induced by ROS in erythrocytes to up-regulate antioxidant genes (Kops et al. 2002; Marinkovic et al. 2007). No changes were observed between exposure groups for WT mice (Figure 4A; Figure S7A,B). PCB-153-exposed SXRKO mice also displayed alterations in the expression of genes involved in glutathione metabolism and synthesis in the spleen compared to DMSO-exposed SXRKO mice, and no differences were observed between exposure groups for WT mice (Figure 4C). PCB-153-exposed SXRKO animals showed higher expression of GSTs, such as microsomal GST 3 (*Mgst3*) (Figure 4C; Figure S7C) and GST pi 3 (*Gstp3*) (Figure 4C; Figure S7D) compared to vehicle-exposed SXRKO mice. No differences were observed between exposure groups for WT mice (Figure S7). RBCs of PCB-153-exposed SXRKO mice also displayed a lower ratio of reduced GSH to total glutathione content compared to DMSO-exposed SXRKO mice (Figure 4D), indicating elevated oxidative stress. RBC membranes of SXRKO mice exposed to PCB-153 showed signs of higher MDA content, indicative of higher lipid peroxidation and oxidative damage, but this did not reach statistical significance (Figure 4B). WT mice displayed no differences in MDA or GSH levels between exposure groups (Figure 4B,D). SXRKO mice exposed to PCB-153 also exhibited altered gene expression of GO terms related to DNA damage in the spleen compared to vehicle-exposed SXRKO mice (Figure S8). These findings support the RNA-seq results pointing toward elevated oxidative stress experienced by SXRKO mice perinatally exposed to PCB-153.

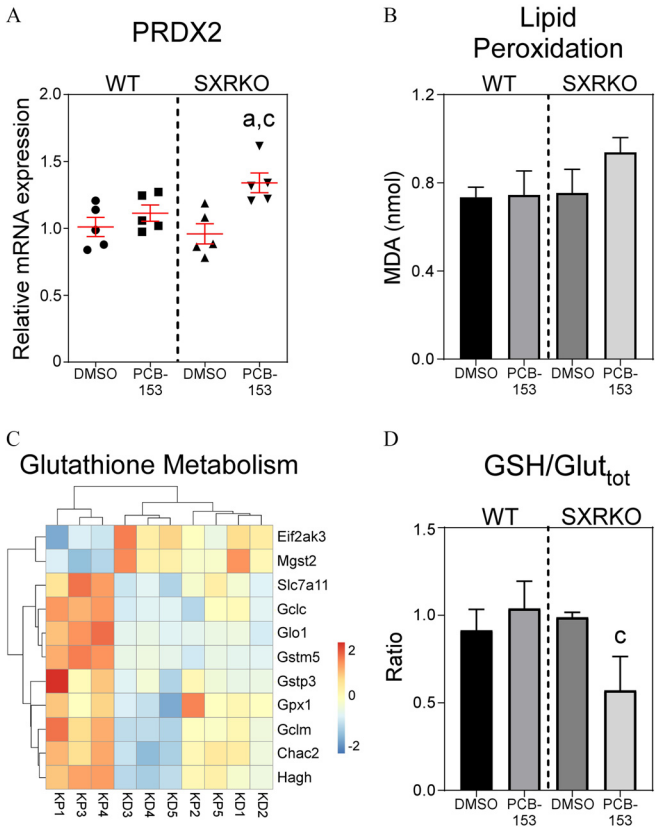

Figure 4. Oxidative stress markers in spleens and red blood cells (RBCs) of 4-wk-old wild-type (WT) and steroid and xenobiotic receptor knockout (SXRKO) mice perinatally exposed to polychlorinated biphenyl 153 (PCB-153) or vehicle. (A) Peroxiredoxin 2 (*Prdx2*) mRNA expression in the spleens of WT and SXRKO mice exposed to PCB-153 or DMSO, plotted as mean fold change over WT dimethylsulfoxide (DMSO) ± standard error of the mean (SEM) ($n = 5$ per group). (B) Malonaldehyde (MDA) levels of RBC membranes from PCB-153- or DMSO-exposed WT and SXRKO mice ($n = 5$ per group); data plotted as mean ± SEM. (C) Heatmap of differentially expressed genes (DEGs) in the spleens between SXRKO mice exposed to PCB-153 ($n = 5$) compared to DMSO ($n = 5$) for genes related glutathione metabolism. (D) Ratio of reduced glutathione (GSH) to total glutathione in RBCs of WT and SXRKO mice exposed to DMSO or PCB-153; plotted as mean ± SEM ($n = 5$ per group). a, statistically significant compared to WT DMSO; c, statistically significant compared to SXRKO DMSO determined by two-way analysis of variance (ANOVA) and Tukey's multiple-comparisons test. Note: D, DMSO exposure; K, SXRKO mice; P, PCB-153 exposure; W, WT mice.

RNA Expression Profile of Metabolism Related Pathways in the Liver of 4-Wk-Old Wild-Type and SXRKO Mice

SXR/PXR is expressed at high levels in the liver, a principal site of xenobiotic metabolism, of several animal species, including mice (Kliewer et al. 1998) and humans (Blumberg et al. 1998). The liver transcriptomes from 4-wk-old WT and SXRKO mice were compared to investigate whether the phenotypic differences were the result of distinct metabolic responses to PCB-153. A low number of DEGs were associated with PCB-153 exposure in the livers of both WT and SXRKO mice compared to their vehicle-exposed counterparts in the RNA-seq data set (Table 2). However, the results revealed inherent differences between livers of WT and SXRKO mice in terms such as xenobiotic metabolism, oxidation–reduction processes, and glutathione metabolic process (Figure 5; Figure S9). These inherent differences included differential expression of many CYP genes. Several isoforms of the CYP2B family of P450s catalyze phase I metabolism of NDL-PCBs (Grimm et al. 2015). Expression of *Cyp2b9* and *Cyp2b10* were elevated in SXRKO mice compared to WT (Figure 5A,B). However, many other CYP genes were down-regulated in SXRKO mice compared to WT (Figure 5A). There appears to be higher *Cyp2b10* expression in the livers of PCB-153-exposed SXRKO mice compared to vehicle-exposed SXRKO mice, but it was not statistically different, and no differences between exposure groups for WT mice were observed (Figure 5B). Several drug/xenobiotic transmembrane transporter genes were also differentially expressed in the liver between WT and SXRKO mice perinatally exposed to PCB-153 (Figure S10A), including the solute carrier (SLC) organic anion transporter family member 1A1 (*Slco1a1*); no differences were observed between exposure groups for either WT or SXRKO mice (Figure S10B). SXRKO mice also showed lower expression of several GSTs, such as *Gstp1* (Figure 5C,D) and higher expression of several sulfotransferases (SULTs), such as *Sult2a1* (Figure S11C,D), in the liver compared to WT controls. These results demonstrated an overall altered metabolism gene expression profile in liver of SXRKO mice compared to WT mice.

Table 2. Liver transcriptome sequencing (RNA-seq) results.

	SXRKO DMSO vs. WT DMSO	SXRKO PCB vs. WT PCB	SXRKO PCB vs. SXRKO DMSO	WT PCB vs. WT DMSO
Total DEGs	260	394	60	0
Up-regulated	142	180	19	0
Down-regulated	118	214	41	0
GO terms (BPs)	47	103	9	0

Note: Number of total, up-regulated, and down-regulated differentially expressed genes (DEGs) for each comparison and the resulting number of significant gene ontology (GO) terms for biological processes (BPs). DEGs were determined by DESeq2 with p-adj <0.05 and absolute value of log2 [fold change (FC)] > 0.3. GO term significance determined by Benjamini-Hochberg correction test (p-adj <0.05) in MouseMine (Mouse Genome Informatics 2019). DMSO, dimethylsulfoxide; PCB, polychlorinated biphenyl-153; SXRKO, steroid and xenobiotic receptor knockout (SXRKO); WT, wild-type.

PCB-153 and 3-OH-PCB-153 Levels in the Plasma and Liver of 4-Wk-Old Wild-Type and SXRKO Mice Perinatally Exposed to PCB-153

We investigated the levels of PCB-153 in the plasma and liver of perinatally exposed WT and SXRKO mice to determine if there were any differences between genotypes. No differences were observed in PCB-153 levels between WT and SXRKO animals for both plasma and liver (Figure 6A,D). However, levels of a major hydroxylated metabolite of PCB-153, 3-OH-PCB-153, were elevated in both the plasma and livers of PCB-153-exposed SXRKO mice compared to PCB-153-exposed WT mice (Figure 6). Expression of many uridine 5′-diphosphate–glucuronyl transferase (UGT) genes, which have been demonstrated to be involved in the conjugation of hydroxylated PCB metabolites (Daidoji et al. 2005; Grimm et al. 2015), was higher in PCB-153-exposed SXRKO mice compared to exposed WT (Figure S11A). One UGT gene, *Ugt3a1*, was down-regulated in unexposed SXRKO mice compared to unexposed WT mice (Figure S11B).

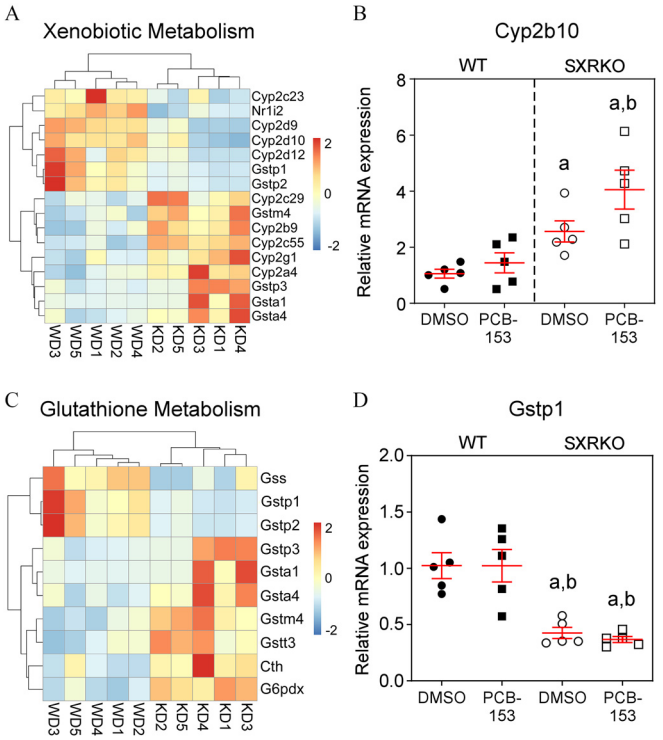

Figure 5. Liver transcriptome sequencing (RNA-seq) results comparing 4-wk-old wild-type (WT) and steroid and xenobiotic receptor knockout (SXRKO) mice. (A) Liver RNA-seq analysis of xenobiotic metabolism differentially expressed genes (DEGs) of vehicle [dimethylsulfoxide (DMSO)]-exposed SXRKO mice compared to vehicle-exposed WT mice. (B) Cytochrome P450 2b10 (*Cyp2b10*) mRNA expression in the liver measured by quantitative real-time polymerase chain reaction (qPCR) ($n = 5$ per group) plotted as mean ± standard error of the mean (SEM). (C) Heatmap of DEGs in the liver between vehicle-exposed SXRKO mice compared to vehicle-exposed WT mice. (D) Liver glutathione S-transferase (GST) pi 1 (Gstp1) mRNA expression measured by qPCR ($n = 5$ per group) plotted as mean ± SEM. a, statistically significant compared to WT DMSO; b, statistically significant compared to WT PCB, determined by two-way analysis of variance (ANOVA) and Tukey's multiple-comparisons test. Note: D, DMSO exposure; K, SXRKO mice; P, PCB-153 exposure; W, WT mice.

Prevalence of Intestinal Tumors in Wild-Type and SXRKO Mice Chronically Exposed to PCB-153

Chronic exposure to PCB-153 (54 μg/kg BW/d) led to the development of tumors in the upper small intestine of SXRKO mice that were observed at 10 months of age. These tumors occurred in approximately 11% (4/35) of the PCB-153-exposed SXRKO mice (Figure 7A) and were located near the jejunum–duodenum junction (Figure 7B; Figure S12A). These results derived from three independent chronic exposure studies, one of which included a hSXRki transgenic mouse strain (Igarashi et al. 2012). No WT or hSXRki mice in either exposure group developed intestinal tumors in any of the studies. The tumors were characterized as intestinal adenocarcinomas with a rare morphology that resembled signet ring cell carcinoma (Figure S12B). Tumor-bearing SXRKO mice chronically exposed to PCB-153 also displayed enlarged spleens accompanied by robustly elevated erythropoiesis (Figure 7C,D; Figure S12C). Ten-month-old SXRKO mice chronically exposed to PCB-153 also displayed lower BWs (Figure S12D), resembling the lower BWs observed at 4 wk of age in the perinatal exposure study (Figure 2F).

Discussion

PCBs are highly persistent environmental contaminants known to cause many detrimental acute and developmental effects in humans and wildlife (Safe 1994). PCB exposure during early development often leads to more severe and longer-lasting effects than does adult exposure (Curran et al. 2011; Guo et al. 1995; Jacobson et al. 1990b). Therefore, determining the underlying molecular mechanisms responsible for the effects elicited by acute, chronic, and developmental exposures and how to protect against them is vital to protect public health. While much is known about the mechanisms through which DL-PCBs act, a large knowledge gap remains concerning the mechanisms of action for NDL-PCBs. This study demonstrated that loss of SXR/PXR resulted in elevated toxicity of PCB-153, likely due to accumulation of metabolites that induce oxidative stress. This highlights the importance of SXR/PXR in the protection against exposure to NDL-PCBs and likely other xenobiotics with reactive metabolites.

Here, we showed that perinatal exposure of SXRKO mice to PCB-153 led to a phenotype resembling hemolytic anemia, a previously unreported effect of exposure to this toxicant. The anemia was characterized by lower HGB levels that persisted throughout the lifespan (Figures 1C and 2E), with elevated compensatory and stress erythropoiesis observed by 4 wk of age (Figure 2A–D). Splenic erythropoiesis is commonly associated with anemia, which

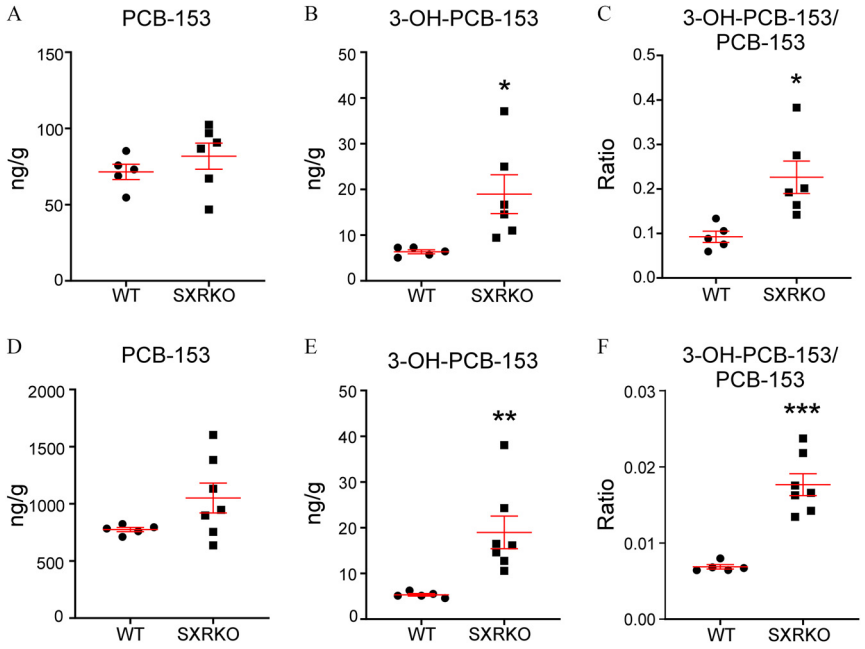

Figure 6. Levels of polychlorinated biphenyl 153 (PCB-153) and the PCB-153 metabolite, 3-OH-PCB-153, in exposed wild-type (WT) and steroid and xenobiotic receptor knockout (SXRKO) mice at 4 wk of age. Levels of (A) PCB-153 and (B) 3-OH-PCB-153 and (C) the ratio of 3-OH-PCB-153 to PCB-153 in the plasma of PCB-153-exposed WT ($n=5$) and SXRKO ($n=6$) mice plotted as mean ± standard error of the mean (SEM). Levels of (D) PCB-153 and (E) 3-OH-PCB-153 and (F) the ratio of 3-OH-PCB-153 to PCB-153 in liver of PCB-153-exposed WT ($n=5$) and SXRKO ($n=7$) mice plotted as mean ± SEM. $^{*}p<0.05$; $^{**}p<0.01$; $^{***}p<0.001$ determined by Student's *t*-test.

results from ineffective medullary erythropoiesis or another form of RBC stress (Bozzini et al. 1970; Paulson et al. 2011). Higher erythropoiesis in PCB-153-exposed SXRKO mice was observed in both the spleens and bone marrow, suggesting that something other than ineffective medullary erythropoiesis was the cause of the anemia. Higher expression of heme catabolic genes, such as *Blvra* and *Blvrb* (Figure 3C,D), is consistent with the possibility that SXRKO mice exposed to PCB-153 also experienced elevated RBC destruction, characteristic of hemolytic anemia (Beutler 1969). The lower HGB values and associated erythropoiesis could be the results of other hematological abnormalities, such as altered RBC morphology or development of dysfunctional HGB, although this was not investigated in our study. Another possibility is that there was undetected blood loss in the gastrointestinal tract of these animals.

ROS and oxidative stress cause cell damage leading to RBC destruction and anemia (Fibach and Rachmilewitz 2008; Han et al. 2012; Iuchi et al. 2010). Oxidative stress–induced hemolytic anemia has been associated with exposure to some xenobiotics and is thought to be caused by altered glutathione synthesis or glutathione

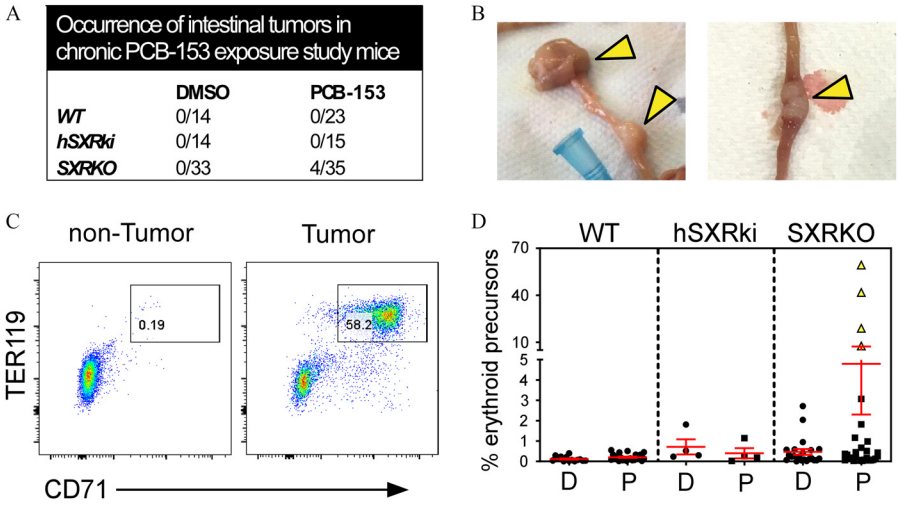

Figure 7. Prevalence and characterization of intestinal tumors in steroid and xenobiotic receptor knockout (SXRKO) mice chronically exposed to polychlorinated biphenyl 153 (PCB-153) until 10 months of age. (A) Number of intestinal tumors found in the upper intestine of 10-month-old wild-type (WT), SXRKO, and human SXR/pregnane X receptor (PXR) knock-in (hSXRki) mice chronically exposed to PCB-153 or dimethylsulfoxide (DMSO). (B) Representative images of the tumors (indicated by yellow arrowheads) located near the duodenum–jejunum junction of the upper intestine. (C) Representative fluorescence-activated cell sorter (FACS) plots of the spleen of a nontumor- vs. tumor-bearing mouse, gating on erythroid precursors. (D) Quantification of erythroid precursor percentage in the spleens of chronically exposed mice (WT DMSO, $n=14$; WT PCB, $n=23$; hSXRki DMSO, $n=4$; hSXRki PCB, $n=4$; SXRKO DMSO, $n=22$; SXRKO PCB, $n=30$) plotted as mean ± standard error of the mean (SEM); tumor-bearing mice are indicated with yellow triangle symbols.

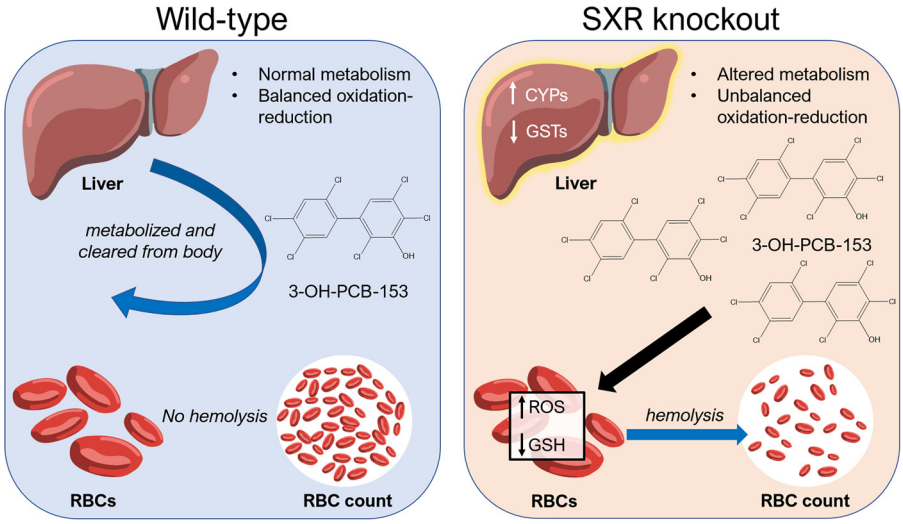

Figure 8. Proposed mechanism of oxidative stress and anemia phenotype induced by polychlorinated biphenyl 153 (PCB-153) in steroid and xenobiotic receptor knockout (SXRKO) mice.

redox cycle regulation (Beutler 1969; Bowman et al. 2004). GSH is a tripeptide that acts as both an antioxidant and detoxifying agent (Meister and Anderson 1983). GSH reduces hydrogen peroxides and other ROS, this process produces the oxidized form of glutathione, GSSG (Townsend et al. 2003). SXRKO mice perinatally exposed to PCB-153 had lower levels of GSH (the reduced form of glutathione) in whole blood, indicating elevated oxidative stress. Here, we also observed higher expression of mRNAs encoding key antioxidants, Gpx1 and Prdx2, which may indicate a physiological compensation to combat the elevated oxidative stress.

In addition to oxidation and reduction, GSH also participates in the detoxification of xenobiotics but requires catalysis by GST. SXRKO mice showed altered expression of mRNAs encoding GSTs in the liver, with lower *Gstp1* and *Gstp2* and higher *Gstp3* expression (Figure 5C,D). GSTs also detoxify harmful metabolites of oxidative stress (Hayes et al. 2005). These differences suggested that SXRKO mice have altered detoxification by GSH, which could have led to elevated levels of oxidative stress–inducing metabolites and lower levels of GSH. This would make SXRKO mice more susceptible to oxidative stress. We observed signs of elevated oxidative stress in the spleens and RBCs of SXRKO mice exposed to PCB-153 (Figure 4). GST deficiencies have been reported in human anemia cohorts (Beutler et al. 1988; Lee et al. 2001). Another study linked GST polymorphisms with sickle cell anemia (Silva et al. 2011).

Transcriptomal analysis of livers revealed inherent differences in gene expression between WT and SXRKO mice, mostly related to xenobiotic metabolism or oxidation–reduction processes (Figure 5; Figure S9); thus, we inferred that there may be resulting differences in PCB-153 metabolism between WT and SXRKO mice. We observed elevated levels of the hydroxylated metabolite of PCB-153, 3-OH-PCB-153, in both the plasma and livers of exposed SXRKO mice compared to exposed WT (Figure 6). Hydroxylated PCB metabolites are known to induce oxidative stress and DNA damage; this mechanism was hypothesized to be responsible for many of their adverse health effects (Al-Anati et al. 2015; Dreiem et al. 2009). Therefore, we propose that the elevated levels of 3-OH-PCB-153 in PCB-153-exposed SXRKO mice resulted in oxidative stress on the RBCs, which induced a phenotype resembling hemolytic anemia (Figure 8). This would also explain why we did not observe direct RBC hemolysis from the parent PCB compound (Figure S6). Elevated 3-OH-PCB-153 levels may have also contributed to the development of tumors in chronically exposed SXRKO mice via an elevated amount ROS and DNA damage, although this has yet to be demonstrated.

PCBs are hydroxylated by various cytochrome P450 or CYP enzymes, although it is thought that the Cyp2b family plays the largest role (Grimm et al. 2015). We observed higher expression of mRNAs encoding *Cyp2b9* and *Cyp2b10* in the livers of SXRKO mice (Figure 5A,B), which could explain the higher level of hydroxylated metabolites in PCB-153-exposed SXRKO mice. The altered expression of GSTs in the liver of SXRKO mice (Figure 5C,D) could also contribute to the elevated levels of OH-PCB153 due to their involvement in the detoxification of arene oxide metabolites of PCBs (Grimm et al. 2015). UGTs are phase II metabolizing enzymes that conjugate a glucuronic acid to the hydroxyl group of hydrophobic compounds to aid in their clearance from the body (Burchell et al. 1989). These enzymes conjugate various OH-PCB metabolites (Daidoji et al. 2005; Grimm et al. 2015). Lower *Ugt3a1* expression in SXRKO mice with both vehicle and PCB-153 exposure (Figure S11B) provides a possible explanation for the elevated levels of 3-OH-PCB-153 metabolite, but our study did not provide any evidence to support this. Many other UGT genes were up-regulated in the livers of PCB-153-exposed SXRKO mice compared to PCB-153-exposed WT mice (Figure S11A).

SULTs are phase II metabolizing enzymes that conjugate a sulfonyl onto a hydroxyl group of xenobiotics to aid in its solubility and clearance (Gamage et al. 2006). SXRKO mice had elevated expression of several SULTs compared to WT controls (Figure S11C,D). This appears to contradict our results of higher accumulation of 3-OH-PCB-153; however, it has been reported that some OH-PCB metabolites can inhibit SULT activity (Liu et al. 2006; Liu et al. 2009). In addition, *Sult1e1* was the only up-regulated SULT gene in PCB-153 exposed SXRKO mice compared to PCB-153-exposed WT mice (Figure S11C), and this specific SULT isoform, along with Sult1a1, has been shown to bind to hydroxylated PCBs (Shevtsov et al. 2003). The higher expression of several UGT genes and Sult1e1 in PCB-153-exposed SXRKO mice is likely a compensatory response to the larger presence of 3-OH-PCB-153. The up-regulation of these enzymes can result in an increase in phase II metabolites of 3-OH-PCB-153, which may also induce oxidative stress.

Another explanation for the elevated levels of 3-OH-PCB-153 in SXRKO mice could be alterations in xenobiotic transport. Decreased transport of PCB-153 and 3-OH-PCB-153 would likely lead to an accumulation of these compounds in the tissues.

We observed differential expression of various transporter genes between WT and SXRKO animals, most notably with PCB-153 exposure (Figure S10). SLC transporters have been reported to transport various environmental contaminants (Fardel et al. 2012), so it is possible that they could be involved in the transport of PCBs. RNA-seq analysis of the livers revealed several SLC genes that were differentially expressed between SXRKO and WT mice during PCB-153 exposure (Figure S10). Many of these SLC genes, including *Slco1a1*/*OATP-1*, were down-regulated in SXRKO mice compared to WT (Figure S10). These findings suggest that impaired transporter activity could have been a major contributing factor to the accumulation of PCB metabolites and thus, the downstream toxic effects.

Our chronic exposure study demonstrated that exposure to PCB-153 *in utero* and until 10 months of age resulted in intestinal tumor development in a subset of SXRKO mice (Figure 7A,B). These tumors were characterized as intestinal adenocarcinomas (Figure S12B). SXRKO mice have previously been reported to develop tumors in multiple tissues, including the intestine, although the tumors were characterized as B-cell lymphomas (Casey et al. 2011). In addition, activation of SXR/PXR was shown to suppress tumorigenicity in a colon cancer cell line (Ouyang et al. 2010) and in a mouse model of colon cancer (Cheng et al. 2014). Conversely, SXR/PXR activation was shown to promote colon cancer aggressiveness in both human colon cancer cell lines and in primary human colon cancers xenografted into immunodeficient mice (Wang et al. 2011). Our results suggest that loss of SXR/PXR resulted in increased susceptibility to tumorigenesis in the upper small intestine in conjunction with exposure to PCB-153. Discrepancies between studies could be due to differences in humans vs. mice or in the tissue (colon vs. upper intestine) being investigated. The tumor-bearing mice in our chronic exposure study also displayed elevated erythropoiesis (Figure 7C,D). Splenic erythropoiesis was reportedly associated with tumor development in mouse models, and it was shown recently that erythroblasts of tumor-bearing mice can further stimulate tumor progression (Han et al. 2018). Since only the tumor-bearing, 10-month-old mice displayed erythropoiesis in our study, we inferred that tumor formation in old, chronically exposed mice may not have been induced by the erythropoiesis we observed in young, perinatally exposed SXRKO mice. Many PCBs and/or their metabolites were reported to be genotoxic, and this is widely believed to be a primary mechanism through which PCB exposure led to cancers (Al-Anati et al. 2015; Oakley et al. 1996; Sandal et al. 2008). Therefore, it is possible that the intestinal tumors observed in PCB-153-exposed SXRKO mice arose due to elevated oxidative stress and genotoxicity elicited by higher levels of 3-OH-PCB-153.

Surprisingly, PCB-153 exposure had no significant effects on the liver transcriptomes of WT mice and only a small effect on the liver transcriptomes of SXRKO mice (Table 2). The lack of induction of typical xenobiotic metabolizing enzymes could possibly be the result of using a dose lower than the NOAEL of PCB-153, which, for mice, is between 1 and 125 mg/kg BW/d, depending on the biological end point (European Food Safety Authority 2005). Other studies showed that doses of 3.6 mg/kg BW/d may be required to observe gene expression differences in the mouse liver (Mesnier et al. 2015). We observed gene expression differences, accompanied by evidence of oxidative stress, symptoms resembling hemolytic anemia, premature lethality, and tumor development with exposure of SXRKO mice to a much lower dose of PCB-153 than in other studies. We propose that the altered metabolism profile of SXRKO mice led to the accumulation of the hydroxylated metabolites of PCB-153, which then elicited these toxic effects (Figure 8). Interestingly, WT mice showed a trend for higher blood HGB levels at 4 wk of age with PCB-153 exposure compared to the lower blood HGB values in SXRKO mice exposed to PCB-153 (Figure 2E), although this trend was not observed at later ages (Figure S1A). We suspect that WT mice may have had a compensatory effect to the PCB-153 exposure at early ages, resulting in higher HGB values. However, the RNA-seq and FACS analyses of WT mice at this age revealed no differences between DMSO- and PCB-153-exposed WT mice in terms of mRNA expression of heme synthesis genes (Figure 3D; Figure S4) or percentage of erythroid precursors (Figure 2B,D).

Our results support the possibility that exposure to PCB-153 during sensitive developmental time periods can lead to hemolytic anemia induced by elevated oxidative stress. Moreover, SXR loss of function increased susceptibility to this effect of PCB-153 via alterations in overall xenobiotic and glutathione metabolism, leading to impaired metabolism and/or clearance of toxic PCB metabolites. We observed lower BWs that coincided with lower blood HGB levels in SXRKO mice perinatally exposed to PCB-153 (Figure 2F), and this was consistently seen with chronic exposure up to 10 months of age (Figure S12D). We speculate that the lower BW at 4 wk of age and premature death at 5 wk of age observed in PCB-153-exposed SXRKO mice (Figure 1B) may be linked directly to the anemia phenotype. Mice experience rapid growth from birth up until 5–6 wk of age, which requires increased production of RBCs (Garcia 1957; Peters and Festing 1990). We infer that anemia became fatal in some mice at 5 wk of age due to an unmet need for RBCs and HGB. Exposure to PCBs *in utero* or during early development was associated with lower birth weight, growth rate, and adolescent BW, and these growth abnormalities have also been associated with anemia (Guo et al. 1995; Jacobson et al. 1990a; Patandin et al. 1998). Therefore, our study revealed anemia as a possible component of the mechanism underlying these adverse effects of prenatal or perinatal PCB exposure. Anemia is a highly underinvestigated outcome in PCB-exposed human cohorts and in laboratory animal exposure studies. Only one study reported an anemia phenotype in rats, and this used a high dose (50 mg/L or 14 μmol/kg/d) of PCB-105, a dioxin-like PCB, for 13 wk of exposure (Chu et al. 1998), more than 50-fold higher than the dose used in our study. A chronic exposure study in rhesus monkeys to a mixture of PCBs led to anemia at a concentration of 200 μg/kg/d (or 0.55 μmol/kg/d) for a period of 27 months or longer (Tryphonas et al. 1986). To our knowledge, we are the first to report anemia as an effect of low-dose perinatal PCB exposure.

We recognize that the results from this study may not apply to all PCBs, or even all NDL-PCBs, because many studies have shown congener-specific effects. However, we believe it is important to investigate PCB-153, since it is the most prevalent congener found in the environment, human tissue, and in breast milk (Faroon et al. 2003; Safe 1994). Many replacement chemicals, such as PBBs and PBDEs, were synthesized following the PCB ban. These chemicals have similar structures and properties to PCBs, and many were demonstrated to induce Cyp gene expression (Pacyniak et al. 2007) and inflammation (Koike et al. 2014) and to interact with SXR (Pacyniak et al. 2007). In addition, hydroxylated metabolites of these chemicals have been demonstrated to induce oxidative stress (An et al. 2011; Ji et al. 2011). Whether SXR plays a key role in the protection against and/or metabolism of these chemicals and their metabolites *in vivo* remains to be investigated in the future.

There are currently 9,451 reported SNPs of human SXR on the NCBI Single Nucleotide Polymorphism Database (dbSNP), many of which can impact the expression of SXR itself and/or that of its target genes (NCBI 2019; Zhang et al. 2008). Polymorphisms in SXR have been linked to many functional consequences, including altered metabolism (Lim et al. 2005), increased inflammation (Dring et al. 2006), and susceptibility to disease (Dring et al. 2006; Karlsen et al. 2006). Some xenobiotics and pharmaceutical drugs

were shown to suppress SXR signaling (Krausova et al. 2011; Smutny and Pavek 2014). Antagonists of SXR are actively being developed to be used as pharmaceutical drugs (Staudinger 2019). Our studies suggest that both genetic and chemical inhibition of SXR might predispose humans to increased oxidative stress and lead to more toxic effects from exposure to PCBs. We expect that SXR is important for the metabolism and clearance of other metabolites of many PCB congeners. SXR is important for the metabolism of many xenobiotics; thus, adverse effects of impaired SXR function may not be exclusive to PCB exposure. SXR is likely to be protective against other drugs and xenobiotics with the potential to produce reactive metabolites. There is evidence that hydroxylated metabolites of other xenobiotics, such as those of the antimalarial agent primaquine, can induce oxidative stress and hemolytic anemia (Bowman et al. 2004). Whether SXR also plays a role in the proper metabolism of these xenobiotics and protection against their reactive metabolites is yet to be investigated, but our results indicated that caution is warranted before inhibiting SXR/PXR function as a general method to promote increased efficacy of drugs that might otherwise be metabolized via an SXR/PXR-dependent process.

Acknowledgments

This work was supported by grants from the NIH (ES021832 and ES021832-03S1 to B.B. and ES05605 and ES013661 to H.J.L.) and PhRMA Foundation (predoctoral fellowship in pharmacology/toxicology to R.J.E.). The authors thank all members of the Blumberg and Lehmler laboratories for their technical assistance, Dr. Ron Evans (Salk Institute) for the gift of the SXR knockout mice, Dr. Jun Kanno (National Institute of Health Sciences, Tokyo, Japan) for the gift of SXR humanized mice, Dr. Rick van Etten (UCI) for advice on the characterization of the hematological phenotype and tumors, and Dr. Robert Edwards (UCI) for pathological characterization of intestinal tumors.

References

Al-Anati L, Viluksela M, Strid A, Bergman Å, Andersson PL, Stenius U, et al. 2015. Hydroxyl metabolite of PCB 180 induces DNA damage signaling and enhances the DNA damaging effect of benzo[a]pyrene. Chem Biol Interact 239:164–173, PMID: 26148434, https://doi.org/10.1016/j.cbi.2015.07.002.

Al-Salman F, Plant N. 2012. Non-coplanar polychlorinated biphenyls (PCBs) are direct agonists for the human pregnane-X receptor and constitutive androstane receptor, and activate target gene expression in a tissue-specific manner. Toxicol Appl Pharmacol 263(1):7–13, PMID: 22664347, https://doi.org/10.1016/j.taap.2012.05.016.

Ampleman MD, Martinez A, DeWall J, Rawn DFK, Hornbuckle KC, Thorne PS. 2015. Inhalation and dietary exposure to PCBs in urban and rural cohorts via congener-specific measurements. Environ Sci Technol 49(2):1156–1164, PMID: 25510359, https://doi.org/10.1021/es5048039.

An J, Li S, Zhong Y, Wang Y, Zhen K, Zhang X, et al. 2011. The cytotoxic effects of synthetic 6-hydroxylated and 6-methoxylated polybrominated diphenyl ether 47 (BDE47). Environ Toxicol 26(6):591–599, PMID: 20549613, https://doi.org/10.1002/tox.20582.

Arena SM, Greeley EH, Halbrook RS, Hansen LG, Segre M. 2003. Biological effects of gestational and lactational PCB exposure in neonatal and juvenile C57BL/6 mice. Arch Environ Contam Toxicol 44(2):272–280, PMID: 12520400, https://doi.org/10.1007/s00244-002-2022-5.

Barañano DE, Rao M, Ferris CD, Snyder SH. 2002. Biliverdin reductase: a major physiologic cytoprotectant. Proc Natl Acad Sci USA 99(25):16093–16098, PMID: 12456881, https://doi.org/10.1073/pnas.252626999.

Barone G, Storelli A, Quaglia NC, Dambrosio A, Garofalo R, Chiumarulo R, et al. 2019. Dioxin and PCB residues in meats from Italy: consumer dietary exposure. Food Chem Toxicol 133:110717, PMID: 31356912, https://doi.org/10.1016/j.fct.2019.110717.

Beutler E. 1969. Drug-induced hemolytic anemia. Pharmacol Rev 21(1):73–103, PMID: 4887725.

Beutler E, Dunning D, Dabe I, Forman L. 1988. Erythrocyte glutathione S-transferase deficiency and hemolytic anemia. Blood 72(1):73–77, PMID: 3390613, https://doi.org/10.1182/blood.V72.1.73.73.

Bhavsar SP, Jackson DA, Hayton A, Reiner EJ, Chen T, Bodnar J. 2007. Are PCB levels in fish from the Canadian Great Lakes still declining? J Great Lakes Res 33(3):592–605, https://doi.org/10.3394/0380-1330(2007)33[592:APLIFF]2.0.CO;2.

Blumberg B, Sabbagh W Jr, Juguilon H, Bolado J Jr, van Meter CM, Ong ES, et al. 1998. SXR, a novel steroid and xenobiotic sensing nuclear receptor. Genes Dev 12(20):3195–3205, PMID: 9784494, https://doi.org/10.1101/gad.12.20.3195.

Bonefeld-Jørgensen EC, Andersen HR, Rasmussen TH, Vinggaard AM. 2001. Effect of highly bioaccumulated polychlorinated biphenyl congeners on estrogen and androgen receptor activity. Toxicology 158(3):141–153, PMID: 11275356, https://doi.org/10.1016/s0300-483x(00)00368-1.

Bowman ZS, Oatis JE Jr, Whelan JL, Jollow DJ, McMillan DC. 2004. Primaquine-induced hemolytic anemia: susceptibility of normal versus glutathione-depleted rat erythrocytes to 5-hydroxyprimaquine. J Pharmacol Exp Ther 309(1):79–85, PMID: 14724225, https://doi.org/10.1124/jpet.103.062984.

Bozzini CE, Barrio Rendo M, Devoto FC, Epper CE. 1970. Studies on medullary and extramedullary erythropoiesis in the adult mouse. Am J Physiol 219(3):724–728, PMID: 5450878, https://doi.org/10.1152/ajplegacy.1970.219.3.724.

Brody JG, Moysich KB, Humblet O, Attfield KR, Beehler GP, Rudel RA. 2007. Environmental pollutants and breast cancer: epidemiologic studies. Cancer 109(suppl 12):2667–2711, PMID: 17503436, https://doi.org/10.1002/cncr.22655.

Burchell B, Coughtrie MWH. 1989. UDP-glucuronosyltransferases. Pharmacology 43(2):261–289, https://doi.org/10.1016/0163-7258(89)90122-8.

Casey SC, Nelson EL, Turco GM, Janes MR, Fruman DA, Blumberg B. 2011. B-1 cell lymphoma in mice lacking the steroid and xenobiotic receptor, SXR. Mol Endocrinol 25(6):933–943, PMID: 21436254, https://doi.org/10.1210/me.2010-0486.

Čechová E, Scheringer M, Seifertová M, Mikeš O, Kroupová K, Kuta J, et al. 2017. Developmental neurotoxicants in human milk: comparison of levels and intakes in three European countries. Sci Total Environ 579:637–645, PMID: 27890414, https://doi.org/10.1016/j.scitotenv.2016.11.046.

Cheng J, Fang ZZ, Nagaoka K, Okamoto M, Qu A, Tanaka N, et al. 2014. Activation of intestinal human pregnane X receptor protects against azoxymethane/dextran sulfate sodium-induced colon cancer. J Pharmacol Exp Ther 351(3):559–567, PMID: 25277138, https://doi.org/10.1124/jpet.114.215913.

Chou SM, Miike T, Payne WM, Davis GJ. 1979. Neuropathology of "spinning syndrome" induced by prenatal intoxication with a PCB in mice. Ann N Y Acad Sci 320:373–395, PMID: 110196, https://doi.org/10.1111/j.1749-6632.1979.tb56619.x.

Chu I, Poon R, Yagminas A, Lecavalier P, Håkansson H, Valli V, et al. 1998. Subchronic toxicity of PCB 105 (2,3,3′,4,4′-pentachlorobiphenyl) in rats. J Appl Toxicol 18(4):285–292, PMID: 9719429, https://doi.org/10.1002/(SICI)1099-1263(199807/08)18:4<285::AID-JAT510>3.0.CO;2-9.

Curran CP, Nebert DW, Genter MB, Patel KV, Schaefer TL, Skelton MR, et al. 2011. In utero and lactational exposure to PCBs in mice: adult offspring show altered learning and memory depending on Cyp1a2 and Ahr genotypes. Environ Health Perspect 119(9):1286–1293, PMID: 21571617, https://doi.org/10.1289/ehp.1002965.

Daidoji T, Gozu K, Iwano H, Inoue H, Yokota H. 2005. UDP-glucuronosyltransferase isoforms catalyzing glucuronidation of hydroxy-polychlorinated biphenyls in rat. Drug Metab Dispos 33(10):1466–1476, PMID: 16006569, https://doi.org/10.1124/dmd.105.004416.

DeKoning EP, Karmaus W. 2000. PCB exposure in utero and via breast milk. A review. J Expo Anal Environ Epidemiol 10(3):285–293, PMID: 10910120, https://doi.org/10.1038/sj.jea.7500090.

Dobin A, Davis CA, Schlesinger F, Drenkow J, Zaleski C, Jha S, et al. 2013. Star: ultrafast universal RNA-seq aligner. Bioinformatics 29(1):15–21, PMID: 23104886, https://doi.org/10.1093/bioinformatics/bts635.

Dreiem A, Rykken S, Lehmler HJ, Robertson LW, Fonnum F. 2009. Hydroxylated polychlorinated biphenyls increase reactive oxygen species formation and induce cell death in cultured cerebellar granule cells. Toxicol Appl Pharmacol 240(2):306–313, PMID: 19631230, https://doi.org/10.1016/j.taap.2009.07.016.

Dring MM, Goulding CA, Trimble VI, Keegan D, Ryan AW, Brophy KM, et al. 2006. The pregnane X receptor locus is associated with susceptibility to inflammatory bowel disease. Gastroenterology 130(2):341–348, PMID: 16472590, https://doi.org/10.1053/j.gastro.2005.12.008.

Elnar AA, Diesel B, Desor F, Feidt C, Bouayed J, Kiemer AK, et al. 2012. Neurodevelopmental and behavioral toxicity via lactational exposure to the sum of six indicator non-dioxin-like-polychlorinated biphenyls (Σ6 NDL-PCBs) in mice. Toxicology 299(1):44–54, PMID: 22595366, https://doi.org/10.1016/j.tox.2012.05.004.

Engel LS, Laden F, Andersen A, Strickland PT, Blair A, Needham LL, et al. 2007. Polychlorinated biphenyl levels in peripheral blood and non-Hodgkin's lymphoma: a report from three cohorts. Cancer Res 67(11):5545–5552, https://doi.org/10.1158/0008-5472.CAN-06-3906.

European Food Safety Authority. 2005. Opinion of the scientific panel on contaminants in the food chain [contam] related to the presence of non dioxin-like polychlorinated biphenyls (PCB) in feed and food. EFSA Journal 3(284):1–137, https://doi.org/10.2903/j.efsa.2005.284.

Evans BC, Nelson CE, Yu SS, Beavers KR, Kim AJ, Li H, et al. 2013. Ex vivo red blood cell hemolysis assay for the evaluation of pH-responsive endosomolytic agents for cytosolic delivery of biomacromolecular drugs. JoVE (73):e50166, PMID: 23524982, https://doi.org/10.3791/50166.

Fardel O, Kolasa E, Le Vee M. 2012. Environmental chemicals as substrates, inhibitors or inducers of drug transporters: implication for toxicokinetics, toxicity and pharmacokinetics. Expert Opin Drug Metab Toxicol 8(1):29–46, PMID: 22176607, https://doi.org/10.1517/17425255.2012.637918.

Faroon OM, Samuel Keith L, Smith-Simon C, De Rosa CT. 2003. *Polychlorinated Biphenyls: Human Health Aspects*. Geneva, Switzerland: World Health Organization.

Fein GG, Jacobson JL, Jacobson SW, Schwartz PM, Dowler JK. 1984. Prenatal exposure to polychlorinated biphenyls: effects on birth size and gestational age. J Pediatr 105(2):315–320, PMID: 6431068, https://doi.org/10.1016/s0022-3476(84)80139-0.

Ferrante MC, Mattace Raso G, Esposito E, Bianco G, Iacono A, Clausi MT, et al. 2011. Effects of non-dioxin-like polychlorinated biphenyl congeners (PCB 101, PCB 153 and PCB 180) alone or mixed on j774a.1 macrophage cell line: modification of apoptotic pathway. Toxicol Lett 202(1):61–68, PMID: 21291966, https://doi.org/10.1016/j.toxlet.2011.01.023.

Ferreira GC. 1999. Ferrochelatase. Int J Biochem Cell Biol 31(10):995–1000, PMID: 10582332, https://doi.org/10.1016/s1357-2725(99)00066-7.

Fibach E, Rachmilewitz E. 2008. The role of oxidative stress in hemolytic anemia. Curr Mol Med 8(7):609–619, PMID: 18991647, https://doi.org/10.2174/156652408786241384.

Gährs M, Roos R, Andersson PL, Schrenk D. 2013. Role of the nuclear xenobiotic receptors CAR and PXR in induction of cytochromes p450 by non-dioxinlike polychlorinated biphenyls in cultured rat hepatocytes. Toxicol Appl Pharmacol 272(1):77–85, PMID: 23770461, https://doi.org/10.1016/j.taap.2013.05.034.

Gamage N, Barnett A, Hempel N, Duggleby RG, Windmill KF, Martin JL, et al. 2006. Human sulfotransferases and their role in chemical metabolism. Toxicol Sci 90(1):5–22, PMID: 16322073, https://doi.org/10.1093/toxsci/kfj061.

Garcia JF. 1957. Changes in blood, plasma and red cell volume in the male rat, as a function of age. Am J Physiol 190(1):19–24, PMID: 13458401, https://doi.org/10.1152/ajplegacy.1957.190.1.19.

Gaspar-Ramírez O, Pérez-Vázquez FJ, Salgado-Bustamante M, González-Amaro R, Hernandez-Castro B, Pérez-Maldonado IN. 2015. DDE and PCB 153 independently induce aryl hydrocarbon receptor (AhR) expression in peripheral blood mononuclear cells. J Immunotoxicol 12(3):266–272, PMID: 25316167, https://doi.org/10.3109/1547691X.2014.960108.

Geick A, Eichelbaum M, Burk O. 2001. Nuclear receptor response elements mediate induction of intestinal MDR1 by rifampin. J Biol Chem 276(18):14581–14587, PMID: 11297522, https://doi.org/10.1074/jbc.M010173200.

Giera S, Bansal R, Ortiz-Toro TM, Taub DG, Zoeller RT. 2011. Individual polychlorinated biphenyl (PCB) congeners produce tissue-and gene-specific effects on thyroid hormone signaling during development. Endocrinology 152(7):2909–2919, PMID: 1540284, https://doi.org/10.1210/en.2010-1490.

Grimm FA, Hu D, Kania-Korwel I, Lehmler HJ, Ludewig G, Hornbuckle KC, et al. 2015. Metabolism and metabolites of polychlorinated biphenyls. Crit Rev Toxicol 45(3):245–272, PMID: 25629923, https://doi.org/10.3109/10408444.2014.999365.

Guo YL, Lambert GH, Hsu C-C. 1995. Growth abnormalities in the population exposed in utero and early postnatally to polychlorinated biphenyls and dibenzofurans. Environ Health Perspect 103(suppl 6):117–122, PMID: 8549457, https://doi.org/10.2307/3432359.

Haave M, Bernhard A, Jellestad FK, Heegaard E, Brattelid T, Lundebye AK. 2011. Long-term effects of environmentally relevant doses of 2,2′,4,4′,5,5′-hexachlorobiphenyl (PCB153) on neurobehavioural development, health and spontaneous behaviour in maternally exposed mice. Behav Brain Funct 7:3, PMID: 21232145, https://doi.org/10.1186/1744-9081-7-3.

Hamers T, Kamstra JH, Cenijn PH, Pencikova K, Palkova L, Simeckova P, et al. 2011. In vitro toxicity profiling of ultrapure non-dioxin-like polychlorinated biphenyl congeners and their relative toxic contribution to PCB mixtures in humans. Toxicol Sci 121(1):88–100, PMID: 21357386, https://doi.org/10.1093/toxsci/kfr043.

Han YH, Kim SU, Kwon TH, Lee DS, Ha HL, Park DS, et al. 2012. Peroxiredoxin II is essential for preventing hemolytic anemia from oxidative stress through maintaining hemoglobin stability. Biochem Biophys Res Commun 426(3):427–432, PMID: 22960070, https://doi.org/10.1016/j.bbrc.2012.08.113.

Han Y, Liu Q, Hou J, Gu Y, Zhang Y, Chen Z, et al. 2018. Tumor-induced generation of splenic erythroblast-like Ter-cells promotes tumor progression. Cell 173(3):634–648.e12, PMID: 29606356, https://doi.org/10.1016/j.cell.2018.02.061.

Hardell L, Andersson SO, Carlberg M, Bohr L, van Bavel B, Lindström G, et al. 2006. Adipose tissue concentrations of persistent organic pollutants and the risk of prostate cancer. J Occup Environ Med 48(7):700–707, PMID: 16832227, https://doi.org/10.1097/01.jom.0000205989.46603.43.

Hayes JD, Flanagan JU, Jowsey IR. 2005. Glutathione transferases. Annu Rev Pharmacol Toxicol 45:51–88, PMID: 15822171, https://doi.org/10.1146/annurev.pharmtox.45.120403.095857.

Hsu PC, Pan MH, Li LA, Chen CJ, Tsai SS, Guo YL. 2007. Exposure in utero to 2,2′,3,3′,4,6′-hexachlorobiphenyl (PCB 132) impairs sperm function and alters testicular apoptosis-related gene expression in rat offspring. Toxicol Appl Pharmacol 221(1):68–75, PMID: 17445852, https://doi.org/10.1016/j.taap.2007.01.027.

Hurst CH, Waxman DJ. 2005. Interactions of endocrine-active environmental chemicals with the nuclear receptor PXR. Toxicol Environ Chem 87(3):299–311, https://doi.org/10.1080/02772240400026781.

Igarashi K, Kitajima S, Aisaki KI, Tanemura K, Taquahashi Y, Moriyama N, et al. 2012. Development of humanized steroid and xenobiotic receptor mouse by homologous knock-in of the human steroid and xenobiotic receptor ligand binding domain sequence. J Toxicol Sci 37(2):373–380, PMID: 22467028, https://doi.org/10.2131/jts.37.373.

Iuchi Y, Kibe N, Tsunoda S, Suzuki S, Mikami T, Okada F, et al. 2010. Implication of oxidative stress as a cause of autoimmune hemolytic anemia in NZB mice. Free Radic Biol Med 48(7):935–944, PMID: 20079426, https://doi.org/10.1016/j.freeradbiomed.2010.01.012.

Jacobson JL, Jacobson SW, Humphrey HE. 1990a. Effects of exposure to PCBs and related compounds on growth and activity in children. Neurotoxicol Teratol 12(4):319–326, PMID: 2118230, https://doi.org/10.1016/0892-0362(90)90050-M.

Jacobson JL, Jacobson SW, Humphrey HE. 1990b. Effects of in utero exposure to polychlorinated biphenyls and related contaminants on cognitive functioning in young children. J Pediatr 116(1):38–45, PMID: 2104928, https://doi.org/10.1016/S0022-3476(05)81642-7.

Jacobson JL, Jacobson SW, Humphrey H. 1990. Effects of in utero exposure to polychlorinated biphenyls and related contaminants on cognitive functioning in young children. J Pediatr 116(1):38–45, PMID: 2104928, https://doi.org/10.1016/S0022-3476(05)81642-7.

Ji K, Choi K, Giesy JP, Musarrat J, Takeda S. 2011. Genotoxicity of several polybrominated diphenyl ethers (PBDEs) and hydroxylated PBDEs, and their mechanisms of toxicity. Environ Sci Technol 45(11):5003–5008, PMID: 21545137, https://doi.org/10.1021/es104344e.

Johns Hopkins University Animal Care and Use Committee. 2019. Species specific information: mouse. http://web.jhu.edu/animalcare/procedures/mouse.html#husbandryfiles/194/mouse.html [accessed 26 August 2019].

Kafafi SA, Afeefy HY, Ali AH, Said HK, Kafafi AG. 1993. Binding of polychlorinated biphenyls to the aryl hydrocarbon receptor. Environ Health Perspect 101(5):422–428, PMID: 8119253, https://doi.org/10.1289/ehp.93101422.

Kania-Korwel I, Duffel MW, Lehmler HJ. 2011. Gas chromatographic analysis with chiral cyclodextrin phases reveals the enantioselective formation of hydroxylated polychlorinated biphenyls by rat liver microsomes. Environ Sci Technol 45(22):9590–9596, PMID: 21966948, https://doi.org/10.1021/es2014727.

Kania-Korwel I, Hornbuckle KC, Peck A, Ludewig G, Robertson LW, Sulkowski WW, et al. 2005. Congener-specific tissue distribution of aroclor 1254 and a highly chlorinated environmental PCB mixture in rats. Environ Sci Technol 39(10):3513–3520, PMID: 15954224, https://doi.org/10.1021/es047987f.

Kania-Korwel I, Shaikh NS, Hornbuckle KC, Robertson LW, Lehmler HJ. 2007. Enantioselective disposition of PCB 136 (2,2′,3,3′,6,6′-hexachlorobiphenyl) in C57BL/6 mice after oral and intraperitoneal administration. Chirality 19(1):56–66, PMID: 17089340, https://doi.org/10.1002/chir.20342.

Karlsen TH, Lie BA, Frøslie KF, Thorsby E, Broomé U, Schrumpf E, et al. 2006. Polymorphisms in the steroid and xenobiotic receptor gene influence survival in primary sclerosing cholangitis. Gastroenterology 131(3):781–787, PMID: 16952547, https://doi.org/10.1053/j.gastro.2006.05.057.

Kliewer SA, Moore JT, Wade L, Staudinger JL, Watson MA, Jones SA, et al. 1998. An orphan nuclear receptor activated by pregnanes defines a novel steroid signaling pathway. Cell 92(1):73–82, PMID: 9489701, https://doi.org/10.1016/s0092-8674(00)80900-9.

Koike E, Yanagisawa R, Takigami H, Takano H. 2014. Penta- and octa-bromodiphenyl ethers promote proinflammatory protein expression in human bronchial epithelial cells in vitro. Toxicol In Vitro 28(2):327–333, PMID: 24184330, https://doi.org/10.1016/j.tiv.2013.10.014.

Kops G, Dansen TB, Polderman PE, Saarloos I, Wirtz KWA, Coffer PJ, et al. 2002. Forkhead transcription factor FOXO3A protects quiescent cells from oxidative stress. Nature 419(6904):316–321, PMID: 12239572, https://doi.org/10.1038/nature01036.

Krausova L, Stejskalova L, Wang H, Vrzal R, Dvorak Z, Mani S, et al. 2011. Metformin suppresses pregnane X receptor (PXR)-regulated transactivation of CYP3A4 gene. Biochem Pharmacol 82(11):1771–1780, PMID: 21920351, https://doi.org/10.1016/j.bcp.2011.08.023.

Lee KA, Kim SH, Woo HY, Hong YJ, Cho HC. 2001. Increased frequencies of glutathione S-transferase (GSTM1 and GSTT1) gene deletions in Korean patients with acquired aplastic anemia. Blood 98(12):3483–3485, PMID: 11719393, https://doi.org/10.1182/blood.v98.12.3483.

Liao Y, Smyth GK, Shi W. 2014. Featurecounts: an efficient general purpose program for assigning sequence reads to genomic features. Bioinformatics 30(7):923–930, PMID: 24227677, https://doi.org/10.1093/bioinformatics/btt656.

Lim YP, Liu CH, Shyu LJ, Huang JD. 2005. Functional characterization of a novel polymorphism of pregnane X receptor, Q158K, in Chinese subjects. Pharmacogenet Genomics 15(5):337–341, PMID: 15864135, https://doi.org/10.1097/01213011-200505000-00009.

Liu Y, Apak TI, Lehmler HJ, Robertson LW, Duffel MW. 2006. Hydroxylated polychlorinated biphenyls are substrates and inhibitors of human hydroxysteroid

sulfotransferase SULT2A1. Chem Res Toxicol 19(11):1420–1425, PMID: 17112228, https://doi.org/10.1021/tx060160+.
Liu Y, Smart JT, Song Y, Lehmler HJ, Robertson LW, Duffel MW. 2009. Structure-activity relationships for hydroxylated polychlorinated biphenyls as substrates and inhibitors of rat sulfotransferases and modification of these relationships by changes in thiol status. Drug Metab Dispos 37(5):1065–1072, PMID: 19196841, https://doi.org/10.1124/dmd.108.026021.
Livak KJ, Schmittgen TD. 2001. Analysis of relative gene expression data using real-time quantitative PCR and the $2-\delta\delta$ct method. Methods 25(4):402–408, PMID: 11846609, https://doi.org/10.1006/meth.2001.1262.
Looser R, Ballschmiter K. 1998. Biomagnification of polychlorinated biphenyls (PCBs) in freshwater fish. Fresenius J Anal Chem 360(7–8):816–819, https://doi.org/10.1007/s002160050816.
Love MI, Huber W, Anders S. 2014. Moderated estimation of fold change and dispersion for RNA-seq data with DESeq2. Genome Biol 15(12):550, PMID: 25516281, https://doi.org/10.1186/s13059-014-0550-8.
Lu Z, Lee EY, Robertson LW, Glauert HP, Spear BT. 2004. Effect of 2,2′,4,4′,5,5′-hexachlorobiphenyl (PCB-153) on hepatocyte proliferation and apoptosis in mice deficient in the p50 subunit of the transcription factor NF-κb. Toxicol Sci 81(1):35–42, PMID: 15201435, https://doi.org/10.1093/toxsci/kfh193.
Lüth A, Lahrssen-Wiederholt M, Karl H. 2018. Studies on the influence of sampling on the levels of dioxins and PCB in fish. Chemosphere 212:1133–1141, PMID: 30286542, https://doi.org/10.1016/j.chemosphere.2018.09.011.
Marinkovic D, Zhang X, Yalcin S, Luciano JP, Brugnara C, Huber T, et al. 2007. Foxo3 is required for the regulation of oxidative stress in erythropoiesis. J Clin Invest 117(8):2133–2144, PMID: 17671650, https://doi.org/10.1172/JCI31807.
Meister A, Anderson ME. 1983. Glutathione. Annu Rev Biochem 52:711–760, PMID: 6137189, https://doi.org/10.1146/annurev.bi.52.070183.003431.
Mesnier A, Champion S, Louis L, Sauzet C, May P, Portugal H, et al. 2015. The transcriptional effects of PCB118 and PCB153 on the liver, adipose tissue, muscle and colon of mice: highlighting of Glut4 and Lipin1 as main target genes for PCB induced metabolic disorders. PLoS One 10(6):e0128847, PMID: 26086818, https://doi.org/10.1371/journal.pone.0128847.
Miki Y, Suzuki T, Tazawa C, Blumberg B, Sasano H. 2005. Steroid and xenobiotic receptor (SXR), cytochrome p450 3a4 and multidrug resistance gene 1 in human adult and fetal tissues. Mol Cell Endocrinol 231(1–2):75–85, PMID: 15713537, https://doi.org/10.1016/j.mce.2004.12.005.
Milanowski B, Lulek J, Lehmler HJ, Kania-Korwel I. 2010. Assessment of the disposition of chiral polychlorinated biphenyls in female mdr 1a/b knockout versus wild-type mice using multivariate analyses. Environ Int 36(8):884–892, PMID: 19923000, https://doi.org/10.1016/j.envint.2009.10.007.
Mouse Genome Informatics. 2019. MouseMine. Updated 31 March 2020. http://www.mousemine.org/mousemine/begin.do [accessed 9 April 2019].
Muir DC, Norstrom RJ, Simon M. 1988. Organochlorine contaminants in arctic marine food chains: accumulation of specific polychlorinated biphenyls and chlordane-related compounds. Environ Sci Technol 22(9):1071–1079, PMID: 22148662, https://doi.org/10.1021/es00174a012.
NCBI. 2019. dbSNP database. https://www.ncbi.nlm.nih.gov/snp/ [accessed 31 May 2019].
Ness DK, Schantz SL, Moshtaghian J, Hansen LG. 1993. Effects of perinatal exposure to specific PCB congeners on thyroid hormone concentrations and thyroid histology in the rat. Toxicol Lett 68(3):311–323, PMID: 8516785, https://doi.org/10.1016/0378-4274(93)90023-q.
Norström K, Czub G, McLachlan MS, Hu D, Thorne PS, Hornbuckle KC. 2010. External exposure and bioaccumulation of PCBs in humans living in a contaminated urban environment. Environ Int 36(8):855–861, PMID: 19394084, https://doi.org/10.1016/j.envint.2009.03.005.
Oakley GG, Devanaboyina US, Robertson LW, Gupta RC. 1996. Oxidative DNA damage induced by activation of polychlorinated biphenyls (PCBs): implications for PCB-induced oxidative stress in breast cancer. Chem Res Toxicol 9(8):1285–1292, PMID: 8951230, https://doi.org/10.1021/tx960103o.
Okey AB, Riddick DS, Harper PA. 1994. The Ah receptor: mediator of the toxicity of 2,3,7,8-tetrachlorodibenzo-p-dioxin (TCDD) and related compounds. Toxicol Lett 70(1):1–22, PMID: 8310450, https://doi.org/10.1016/0378-4274(94)90139-2.
Ouyang N, Ke S, Eagleton N, Xie Y, Chen G, Laffins B, et al. 2010. Pregnane X receptor suppresses proliferation and tumourigenicity of colon cancer cells. Br J Cancer 102(12):1753–1761, PMID: 20531417, https://doi.org/10.1038/sj.bjc.6605677.
Pacyniak EK, Cheng X, Cunningham ML, Crofton K, Klaassen CD, Guo GL. 2007. The flame retardants, polybrominated diphenyl ethers, are pregnane X receptor activators. Toxicol Sci 97(1):94–102, PMID: 17324954, https://doi.org/10.1093/toxsci/kfm025.
Patandin S, Koopman-Esseboom C, de Ridder MA, Weisglas-Kuperus N, Sauer PJ. 1998. Effects of environmental exposure to polychlorinated biphenyls and dioxins on birth size and growth in Dutch children. Pediatr Res 44(4):538–545, PMID: 9773843, https://doi.org/10.1203/00006450-199810000-00012.
Paulson RF, Shi L, Wu DC. 2011. Stress erythropoiesis: new signals and new stress progenitor cells. Curr Opin Hematol 18(3):139–145, PMID: 21372709, https://doi.org/10.1097/MOH.0b013e32834521c8.
Peters A, Festing M. 1990. Population density and growth rate in laboratory mice. Lab Anim 24(3):273–279, PMID: 2395324, https://doi.org/10.1258/002367790780866227.
Pirard C, Compere S, Firquet K, Charlier C. 2018. The current environmental levels of endocrine disruptors (mercury, cadmium, organochlorine pesticides and PCBs) in a Belgian adult population and their predictors of exposure. Int J Hyg Environ Health 221(2):211–222, PMID: 29146212, https://doi.org/10.1016/j.ijheh.2017.10.010.
Rasmussen JB, Rowan DJ, Lean DRS, Carey JH. 1990. Food chain structure in Ontario lakes determines PCB levels in lake trout (Salvelinus namaycush) and other pelagic fish. Can J Fish Aquat Sci 47(10):2030–2038, https://doi.org/10.1139/f90-227.
Safe SH. 1994. Polychlorinated biphenyls (PCBs): environmental impact, biochemical and toxic responses, and implications for risk assessment. Crit Rev Toxicol 24(2):87–149, PMID: 8037844, https://doi.org/10.3109/10408449409049308.
Safe S, Bandiera S, Sawyer T, Robertson L, Safe L, Parkinson A, et al. 1985. PCBs: structure–function relationships and mechanism of action. Environ Health Perspect 60:47–56, PMID: 2992927, https://doi.org/10.1289/ehp.856047.
Sandal S, Yilmaz B, Carpenter DO. 2008. Genotoxic effects of PCB 52 and PCB 77 on cultured human peripheral lymphocytes. Mutat Res 654(1):88–92, PMID: 18573685, https://doi.org/10.1016/j.mrgentox.2008.05.005.
Shevtsov S, Petrotchenko EV, Pedersen LC, Negishi M. 2003. Crystallographic analysis of a hydroxylated polychlorinated biphenyl (OH-PCB) bound to the catalytic estrogen binding site of human estrogen sulfotransferase. Environ Health Perspect 111(7):884–888, PMID: 12782487, https://doi.org/10.1289/ehp.6056.
Siatecka M, Bieker JJ. 2011. The multifunctional role of EKLF/KLF1 during erythropoiesis. Blood 118(8):2044–2054, PMID: 21613252, https://doi.org/10.1182/blood-2011-03-331371.
Silva DGH, Belini Junior E, de Souza Torres L, Júnior OR, de Castro Lobo C, Bonini-Domingos CR, et al. 2011. Relationship between oxidative stress, glutathione S-transferase polymorphisms and hydroxyurea treatment in sickle cell anemia. Blood Cells Mol Dis 47(1):23–28, PMID: 21489839, https://doi.org/10.1016/j.bcmd.2011.03.004.
Smutny T, Pavek P. 2014. Resveratrol as an inhibitor of pregnane X receptor (PXR): another lesson in PXR antagonism. J Pharmacol Sci 126(2):177–178, PMID: 25341568, https://doi.org/10.1254/jphs.14001lt.
Spinelli JJ, Ng CH, Weber JP, Connors JM, Gascoyne RD, Lai AS, et al. 2007. Organochlorines and risk of non-Hodgkin lymphoma. Int J Cancer 121(12):2767–2775, PMID: 17722095, https://doi.org/10.1002/ijc.23005.
Staudinger JL. 2019. Clinical applications of small molecule inhibitors of Pregnane X receptor. Mol Cell Endocrinol 485:61–71, PMID: 30726709, https://doi.org/10.1016/j.mce.2019.02.002.
Strathmann J, Schwarz M, Tharappel JC, Glauert HP, Spear BT, Robertson LW, et al. 2006. Pcb 153, a non-dioxin–like tumor promoter, selects for β-catenin (Catnb)-mutated mouse liver tumors. Toxicol Sci 93(1):34–40, PMID: 16782779, https://doi.org/10.1093/toxsci/kfl041.
Supek F, Bošnjak M, Škunca N, Šmuc T. 2011. REVIGO summarizes and visualizes long lists of gene ontology terms. PLoS One 6(7):e21800, PMID: 21789182, https://doi.org/10.1371/journal.pone.0021800.
Tabb MM, Kholodovych V, Grün F, Zhou C, Welsh WJ, Blumberg B. 2004. Highly chlorinated PCBs inhibit the human xenobiotic response mediated by the steroid and xenobiotic receptor (SXR). Environ Health Perspect 112(2):163–169, PMID: 14754570, https://doi.org/10.1289/ehp.6560.
Townsend DM, Tew KD, Tapiero H. 2003. The importance of glutathione in human disease. Biomed Pharmacother 57(3–4):145–155, PMID: 12818476, https://doi.org/10.1016/s0753-3322(03)00043-x.
Tryphonas L, Arnold DL, Zawidzka Z, Mes J, Charbonneau S, Wong J. 1986. A pilot study in adult rhesus monkeys (M. mulatta) treated with aroclor 1254 for two years. Toxicol Pathol 14(1):1–10, PMID: 3086960, https://doi.org/10.1177/019262338601400101.
U.S. EPA (U.S. Environmental Protection Agency). 1979. EPA bans PCB manufacture; phases out uses. 19 April 1979. https://archive.epa.gov/epa/aboutepa/epa-bans-pcb-manufacture-phases-out-uses.html [accessed 22 May 2019].
U.S. EPA. 2015. Learn about polychlorinated biphenyls (PCBs). https://www.epa.gov/PCBs/learn-about-polychlorinated-biphenyls-PCBs [accessed 29 May 2019].
van den Berg M, Kypke K, Kotz A, Tritscher A, Lee SY, Magulova K, et al. 2017. WHO/UNEP global surveys of PCDDs, PCDFs, PCBs and DDTs in human milk and benefit–risk evaluation of breastfeeding. Arch Toxicol 91(1):83–96, PMID: 27438348, https://doi.org/10.1007/s00204-016-1802-z.
Verner MA, Hart JE, Sagiv SK, Bellinger DC, Altshul LM, Korrick SA. 2015. Measured prenatal and estimated postnatal levels of polychlorinated biphenyls (PCBs) and ADHD-related behaviors in 8-year-old children. Environ Health Perspect 123(9):888–894, PMID: 25769180, https://doi.org/10.1289/ehp.1408084.

Wang H, Venkatesh M, Li H, Goetz R, Mukherjee S, Biswas A, et al. 2011. Pregnane X receptor activation induces FGF19-dependent tumor aggressiveness in humans and mice. J Clin Invest 121(8):3220–3232, PMID: 21747170, https://doi.org/10.1172/JCI41514.

Wei P, Zhang J, Dowhan D, Han Y, Moore DD. 2002. Specific and overlapping functions of the nuclear hormone receptors CAR and PXR in xenobiotic response. Pharmacogenomics J 2(2):117–126, PMID: 12049174, https://doi.org/10.1038/sj.tpj.6500087.

Weisglas-Kuperus N, Sas TCJ, Koopman-Esseboom C, Van Der Zwan CW, De Ridder MAJ, Beishuizen A, et al. 1995. Immunologic effects of background prenatal and postnatal exposure to dioxins and polychlorinated biphenyls in Dutch infants. Pediatr Res 38(3):404–410, PMID: 7494667, https://doi.org/10.1203/00006450-199509000-00022.

Weisglas-Kuperus N, Vreugdenhil HJ, Mulder PG. 2004. Immunological effects of environmental exposure to polychlorinated biphenyls and dioxins in Dutch school children. Toxicol Lett 149(1–3):281–285, PMID: 15093274, https://doi.org/10.1016/j.toxlet.2003.12.039.

Wu X, Pramanik A, Duffel MW, Hrycay EG, Bandiera SM, Lehmler HJ, et al. 2011. 2,2′,3,3′,6,6′-hexachlorobiphenyl (PCB 136) is enantioselectively oxidized to hydroxylated metabolites by rat liver microsomes. Chem Res Toxicol 24(12):2249–2257, PMID: 22026639, https://doi.org/10.1021/tx200360m.

Xie W, Barwick JL, Downes M, Blumberg B, Simon CM, Nelson MC, et al. 2000a. Humanized xenobiotic response in mice expressing nuclear receptor SXR. Nature 406(6794):435–439, PMID: 10935643, https://doi.org/10.1038/35019116.

Xie W, Barwick JL, Simon CM, Pierce AM, Safe S, Blumberg B, et al. 2000b. Reciprocal activation of xenobiotic response genes by nuclear receptors SXR/PXR and CAR. Genes Dev 14(23):3014–3023, PMID: 11114890, https://doi.org/10.1101/gad.846800.

Zhang B, Xie W, Krasowski MD. 2008. PXR: a xenobiotic receptor of diverse function implicated in pharmacogenetics. Pharmacogenomics 9(11):1695–1709, PMID: 19018724, https://doi.org/10.2217/14622416.9.11.1695.